Influences on the Design and Purification of Soluble, Recombinant Native-Like HIV-1 Envelope Glycoprotein Trimers

Rajesh P. Ringe,[a] Anila Yasmeen,[a] Gabriel Ozorowski,[b] Eden P. Go,[c] Laura K. Pritchard,[d] Miklos Guttman,[e] Thomas A. Ketas,[a] Christopher A. Cottrell,[b] Ian A. Wilson,[b,f] Rogier W. Sanders,[a,g] Albert Cupo,[a] Max Crispin,[d] Kelly K. Lee,[e] Heather Desaire,[c] Andrew B. Ward,[b] P. J. Klasse,[a] John P. Moore[a]

Department of Microbiology and Immunology, Weill Medical College of Cornell University, New York, New York, USA[a]; Department of Integrative Structural and Computational Biology, IAVI Neutralizing Antibody Center, and Center for HIV/AIDS Vaccine Immunology and Immunogen Discovery, The Scripps Research Institute, La Jolla, California, USA[b]; Department of Chemistry, University of Kansas, Lawrence, Kansas, USA[c]; Oxford Glycobiology Institute, Department of Biochemistry, University of Oxford, Oxford, United Kingdom[d]; Department of Medicinal Chemistry, University of Washington, Seattle, Washington, USA[e]; The Skaggs Institute for Chemical Biology, The Scripps Research Institute, La Jolla, California, USA[f]; Department of Medical Microbiology, Academic Medical Center, University of Amsterdam, Amsterdam, The Netherlands[g]

ABSTRACT

We have investigated factors that influence the production of native-like soluble, recombinant trimers based on the *env* genes of two isolates of human immunodeficiency virus type 1 (HIV-1), specifically 92UG037.8 (clade A) and CZA97.012 (clade C). When the recombinant trimers based on the *env* genes of isolates 92UG037.8 and CZA97.012 were made according to the SOSIP.664 design and purified by affinity chromatography using broadly neutralizing antibodies (bNAbs) against quaternary epitopes (PGT145 and PGT151, respectively), the resulting trimers are highly stable and they are fully native-like when visualized by negative-stain electron microscopy. They also have a native-like (i.e., abundant) oligomannose glycan composition and display multiple bNAb epitopes while occluding those for nonneutralizing antibodies. In contrast, uncleaved, histidine-tagged Foldon (Fd) domain-containing gp140 proteins (gp140$_{UNC}$-Fd-His), based on the same *env* genes, very rarely form native-like trimers, a finding that is consistent with their antigenic and biophysical properties and glycan composition. The addition of a 20-residue flexible linker (FL20) between the gp120 and gp41 ectodomain (gp41$_{ECTO}$) subunits to make the uncleaved 92UG037.8 gp140-FL20 construct is not sufficient to create a native-like trimer, but a small percentage of native-like trimers were produced when an I559P substitution in gp41$_{ECTO}$ was also present. The further addition of a disulfide bond (SOS) to link the gp120 and gp41 subunits in the uncleaved gp140-FL20-SOSIP protein increases native-like trimer formation to ~20 to 30%. Analysis of the disulfide bond content shows that misfolded gp120 subunits are abundant in uncleaved CZA97.012 gp140$_{UNC}$-Fd-His proteins but very rare in native-like trimer populations. The design and stabilization method and the purification strategy are, therefore, all important influences on the quality of trimeric Env proteins and hence their suitability as vaccine components.

IMPORTANCE

Soluble, recombinant multimeric proteins based on the HIV-1 *env* gene are current candidate immunogens for vaccine trials in humans. These proteins are generally designed to mimic the native trimeric envelope glycoprotein (Env) that is the target of virus-neutralizing antibodies on the surfaces of virions. The underlying hypothesis is that an Env-mimetic protein may be able to induce antibodies that can neutralize the virus broadly and potently enough for a vaccine to be protective. Multiple different designs for Env-mimetic trimers have been put forth. Here, we used the CZA97.012 and 92UG037.8 *env* genes to compare some of these designs and determine which ones best mimic virus-associated Env trimers. We conclude that the most widely used versions of CZA97.012 and 92UG037.8 oligomeric Env proteins do not resemble the trimeric Env glycoprotein on HIV-1 viruses, which has implications for the design and interpretation of ongoing or proposed clinical trials of these proteins.

Recombinant, soluble envelope glycoprotein (Env) gp140 trimers from human immunodeficiency virus type 1 (HIV-1) are being designed, developed, and produced as vaccine candidates intended to induce neutralizing antibody (NAb) responses (1–8). In general, the goal of trimer design projects is to produce proteins that can be expressed and purified in sufficient quantities for vaccine use while retaining as closely as possible a conformation that mimics functional Env on the surfaces of virus particles. There, Env trimers mediate virus entry into target cells by undergoing a complex and coordinated series of receptor-mediated conformational changes and rearrangements in their gp120 and gp41 subunits that drive the fusion of the viral and cell membranes (9, 10). The fact that they must undergo such structural alterations means that HIV-1 Env trimers are metastable; the constituent subunits

are associated via noncovalent interactions that can be disrupted fairly easily, for example by detergents or modestly elevated temperatures [11, 12]. That inherent instability has repercussions when recombinant versions are made as soluble proteins for vaccine research. Thus, the truncations necessary to produce soluble gp140 proteins (gp140s), which eliminate the membrane-spanning and cytoplasmic domains, further destabilize the trimers such that they disintegrate into the constituent gp120 and gp41 ectodomain (gp41$_{ECTO}$) components.

It is important that recombinant trimers retain a native-like structure because they are intended to raise NAbs that recognize the functional Env trimer on the virus, and hence inhibit virus infection. Although nonnative forms of Env can induce NAbs against neutralization-sensitive viruses (tier 1 classification), they have not been able to raise antibodies that neutralize the more-resistant variants (tier 2 or 3) that are transmitted between people [2, 4, 5, 13–16]. As the paramount goal of most current Env vaccine design strategies is to induce antibodies that possess both potency against tier 2 viruses and breadth against many circulating HIV-1 strains, advances are needed. It can be hypothesized, and now shown, that native-like Env trimers constitute such a step forward by better presenting key epitopes for broadly neutralizing antibodies (bNAbs) that recognize properly folded and assembled quaternary structures [1, 8, 17–26]. How, then, can such native-like trimers be produced and purified most easily? Clearly, this cannot happen without introducing sequence modifications that improve trimer stability.

One successful stabilization strategy involves facilitating the natural cleavage of gp140 into gp120 and gp41$_{ECTO}$, creating an intrasubunit disulfide bond (designated SOS) to covalently link the two subunits, and inserting a point substitution, I559P, into gp41$_{ECTO}$ to maintain the trimer in its prefusion form. The resulting, cleaved, soluble trimers, designated SOSIP.664, when based on a subset of *env* genes such as BG505 and B41, retain native-like structure as assessed by multiple criteria [11, 18, 19, 21, 22, 25–30]. An alternative approach widely used over the past 20 years has been to eliminate the natural cleavage site between gp120 and gp41$_{ECTO}$, such that the two subunits remain covalently linked. Often, a trimerization domain is added to the C terminus of gp41$_{ECTO}$, most commonly a Foldon (Fd) moiety [2, 4, 14, 15, 30–34]. The resulting uncleaved gp140 (gp140$_{UNC}$) proteins can be purified as entities that contain three gp120 subunits and three gp41$_{ECTO}$ subunits [2, 4, 14, 15, 32–36]. However, a variety of assays show that these gp140$_{UNC}$ proteins do not adopt or retain a native-like structure [19, 30, 33, 37–39]. Instead, they represent semidisintegrated trimers in which the uncleaved peptide linking the gp120 and gp41$_{ECTO}$ subunits holds the components together in a disordered fashion [19, 30, 33, 37–41]. Recent reports show that this defect can be at least partially overcome for some Env genotypes by introducing a flexible linker between the C terminus of gp120 and the N terminus of gp41$_{ECTO}$, such that the two subunits remain covalently linked but now in a way that allows them to interact properly [3, 7]. When the I559P substitution is also present, the resulting uncleaved gp140s trimerize and now can adopt a native-like structure that is broadly comparable to those of cleaved SOSIP.664 trimers [3, 7]. Addition of the SOS intermolecular disulfide bond confers additional benefit [7]. These uncleaved, native-like trimers have been designated single-chain gp140 (sc-gp140) or native flexibly linked gp140 (NFL-gp140) [3, 7].

It has been claimed, however, that the introduction of a 20-residue flexible linker (FL20), without any further modification, is sufficient to make fully native-like uncleaved 92UG037.8 gp140-FL20 trimers and that the latter proteins are, in practice, structurally and biophysically comparable to both gp140$_{UNC}$ proteins of the standard design and to cleaved BG505 SOSIP.664 trimers [42]. We have, therefore, explored the basis of these claims by making gp140$_{UNC}$ proteins, with and without a flexible linker, and comparing them to SOSIP.664 trimers made from the same *env* genes, 92UG037.8 and CZA97.012 from clades A and C, respectively. We studied the resulting Env proteins in multiple assay systems, including surface plasmon resonance (SPR), negative-stain electron microscopy (EM), differential scanning calorimetry (DSC), glycan composition analysis, hydrogen/deuterium exchange mass spectrometry (HDX-MS), and disulfide bond profiling. Our conclusion is that the introduction of a flexible linker does not allow native-like trimers to be produced unless either one or both of the I559P and SOS changes are also present. Accordingly, we cannot independently verify the report that the 92UG037.8 and CZA97.012 standard uncleaved gp140 proteins and the flexible linker-containing 92UG037.8 gp140-FL20 variant form predominantly native-like trimers [42]. We also describe how affinity purification strategies, including the use of different bNAb columns, influence the production of fully native-like trimers, as opposed to mixtures of native-like and nonnative forms. Finally, we describe the successful production and some of the properties of fully native-like SOSIP.664 trimers based on the 92UG037.8 and CZA97.012 *env* genes. It is noteworthy that native-like CZA97.012 SOSIP.664-His trimers are almost entirely free of gp120 subunits that are misfolded as a result of disulfide bond scrambling, which in contrast are abundant in the uncleaved CZA97.012 gp140 proteins. These two new SOSIP.664 trimers will be evaluated further as both immunogens and structural substrates.
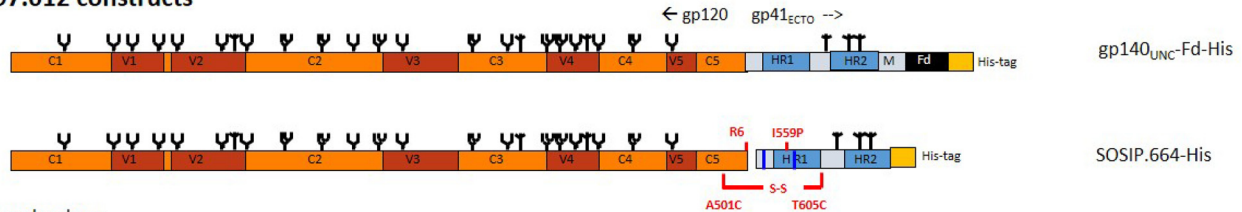
MATERIALS AND METHODS

Env protein design. The designs of the various Env proteins described in this report are summarized in Fig. 1. The CZA97.012 and 92UG037.8 *env* gene sequences and plasmids expressing the gp140$_{UNC}$-Fd-His proteins were obtained from B. Chen (Harvard University) and are the basis of the uncleaved gp140 proteins described in multiple publications [2, 4, 34, 42, 43]. In some reports, the same genes or proteins have sometimes been referred to as C97ZA012, 97ZA012, UG037, UG37, etc. The gp140$_{UNC}$-Fd-His proteins contain the gp120 subunit linked to gp41$_{ECTO}$ via an uncleaved peptide. The gp41$_{ECTO}$ subunit terminates after residue 683, which is immediately followed by the Fd domain and then a six-histidine residue affinity purification tag. The 92UG037.8 gp140-FL20 construct is based on gp140$_{UNC}$-Fd-His but contains a 20-residue flexible linker (FL20) (SGGGG repeated four times) between the C terminus of gp120 and the N terminus of gp41$_{ECTO}$, exactly as described previously [42]. The I559P change was made to this construct to create gp140-FL20-IP, and both the I559P change and the substitutions needed to introduce the intersubunit disulfide bond (A501C plus T605C) were added to make gp140-FL20-SOSIP (Fig. 1).

The CZA97.012 and 92UG037.8 SOSIP.664-His constructs were made by cloning the corresponding *env* genes into the pPPI4 expression vector and then making the following changes, as described previously [18, 28]. The natural leader sequence was replaced with the tissue plasminogen activator leader, the A501C, T605C, and I559P substitutions were added, the REKR cleavage site at residues 508 to 511 was replaced with the RR RRRR sequence, and gp41$_{ECTO}$ was terminated at residue 664, which was followed by a single Gly and then the six-histidine affinity tag. In addition, the 92UG037.8 construct contains an I535M substitution, and the
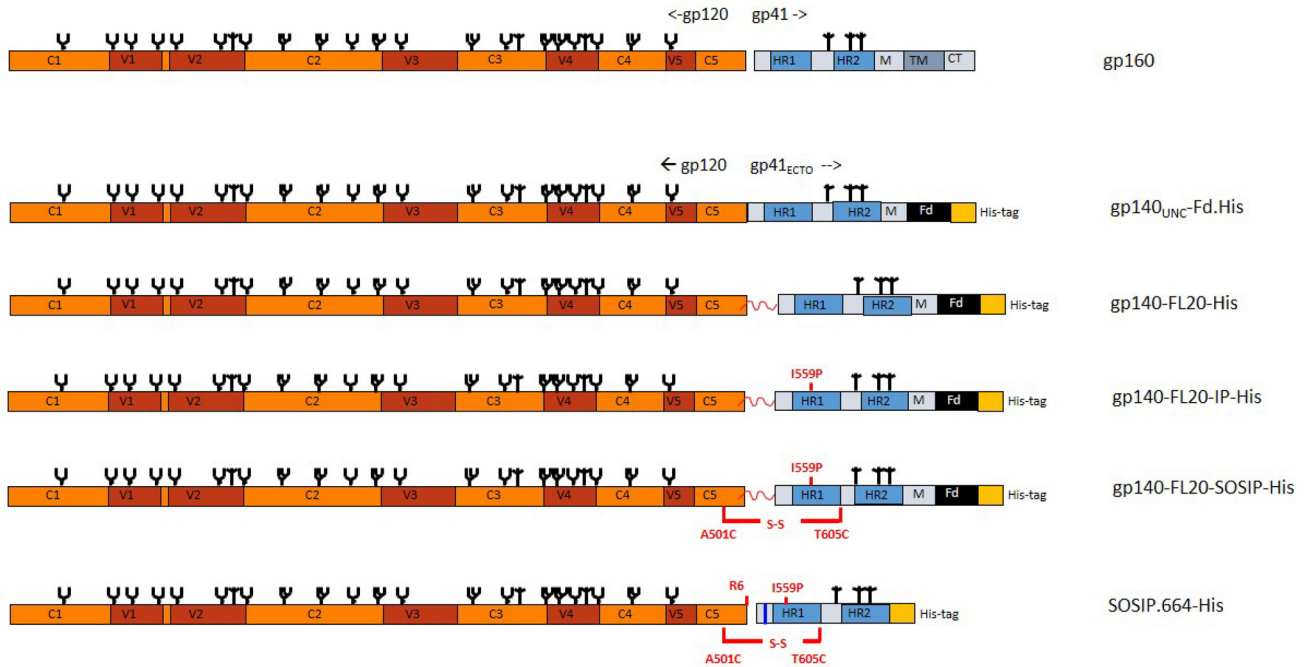
FIG 1 Schematic representations of Env proteins. Linear representations of the 92UG037.8- and CZA97.012-based Env proteins used in these studies are shown, with variable and conserved domains (conserved domain 1 [C1] to C5 and variable domain 1 [V1] to V5) and the positions and classifications of glycan moieties indicated. The following elements are on all the constructs: heptad repeat 1 (HR1), heptad repeat 2 (HR2), and membrane-proximal external region (M). The full-length gp160 protein, not made in this study, contains transmembrane (TM) and cytoplasmic domains that are absent from the soluble proteins. The SOSIP.664-His constructs contain the intersubunit (gp120-gp41$_{ECTO}$) disulfide bond (A501C plus T605C), the I559P substitution, and R6 cleavage-enhancing change, all shown in red. Compared to the 92UG037.8 virus sequence, the corresponding SOSIP.664-His trimer also contains an amino acid substitution, I535M, shown in blue. Similarly, the additional substitutions in the CZA97.012 SOSIP.664-His trimer, also shown in blue, are L535M and Q567K. These changes are not present in the corresponding uncleaved gp140$_{UNC}$-Fd-His proteins. The Foldon (Fd) domains present in the uncleaved gp140s are black, and the His tags are yellow. The 20-residue flexible linkers (FL20s) added to the 92UG037.8 gp140-FL20, gp140-FL20-IP, and gp140-FL20-SOSIP constructs are red, as are the IP and SOSIP changes present in the latter two constructs.

CZA97.012 construct contains the L535M and Q567K changes, which improve trimer formation and expression (unpublished data based on work in reference 44).

Env protein expression and purification. The various CZA97.012 and 92UG037.8 Env proteins were expressed by transient transfection of 293F cells, essentially as previously described (28). The gp140$_{UNC}$-Fd-His, gp140-FL20, gp140-FL20-IP, and gp140-FL20-SOSIP proteins were isolated from culture supernatants via their His tags, using nickel-nitrilotriacetic acid (Ni-NTA) affinity columns and elution with 250 mM imidazole, essentially as recommended by the manufacturer (Life Technologies Inc.) (2, 42). The SOSIP.664-His proteins were purified from culture supernatants using affinity columns containing either *Galanthus nivalis* agglutinin (GNA)-lectin or one of the 2G12, PGT145, or PGT151 bNAbs, and then similarly fractionated by size exclusion chromatography (SEC) (18, 45). The affinity columns were made using a CNBr-activated Sephar-

ose 4B resin (GE Healthcare) as previously described (18). In each case, the culture supernatant was passed through the column at a constant rate of 1 ml/min, the beads were washed with buffer (20 mM Tris-HCl, 500 mM NaCl [pH 8]), and the Env proteins were eluted with 3 M MgCl$_2$ (pH 7.2). The eluted proteins were immediately buffer exchanged into 10 mM Tris-HCl–75 mM NaCl (pH 8) and concentrated using a 100-kDa-cutoff Vivaspin column (GE Healthcare). SEC was used to size fractionate the affinity-purified proteins on a Superdex 200 26/60 column with the same buffer. The isolated trimer fractions were pooled, concentrated, and stored at −80°C.

SDS-PAGE and blue native PAGE. Purified Env proteins were analyzed using 4 to 12% Bis-Tris NuPAGE SDS-PAGE or blue native PAGE (BN-PAGE) gel systems (Invitrogen), followed by Coomassie blue staining. To analyze cleavage, the proteins were incubated for 10 min at room temperature with 0.1 mM dithiothreitol (DTT) before

they were loaded onto the SDS-polyacrylamide gels. BN-polyacryl-amide gels were used to analyze the trimer fractions derived from SEC column runs.

Protease digestion. Purified Env proteins (4 μg) were incubated with a range of concentrations of trypsin, chymotrypsin or proteinase K (all from Sigma) for 1 h at 37°C before analysis by reducing SDS-PAGE (with DTT) as described above.

Antibodies. Monoclonal antibodies (MAbs) were obtained as gifts or purchased from the following sources (shown in parentheses): VRC01 and F105 (John Mascola); PG9, PG16, PGT122, PGT128, PGT135, PGT145, PGT151, b6, b12, and F240 (International AIDS Vaccine Initiative); 2G12 (Polymun Scientific); 3BNC60 and 8ANC195 (Michel Nussenzweig); 39F, 17b, 19b, and 14e (James Robinson); 35O22 (Mark Connors); and CH103 (Barton Haynes).

Surface plasmon resonance. Surface plasmon resonance (SPR) assays were carried out as described previously (26). Briefly, purified His-tagged Env proteins were captured onto CM5 chips by an anti-His MAb (GE Healthcare), which was covalently immobilized in an amount yielding ~15,000 response units (RU). Since Env proteins with and without the Foldon moiety differ by <5% in total mass, we sought to immobilize all Env proteins in amounts yielding similar signals (mean, 527 RU; 95% confidence interval [95% CI] of mean, 525 to 530 RU). The CD4-IgG2 protein and all the MAbs except 2G12 were then injected at a concentration of 500 nM. The 2G12 MAb was injected at 62 nM, because we found that when it was added at 500 nM, it bound Env proteins at levels that are greater than the expected stoichiometry of one IgG per gp120. This outcome may reflect a second, lower-affinity interaction between 2G12 and Env (46, 47). The flow rate was 50 μl/min throughout the MAb association and dissociation phases. After each cycle of MAb association and dissociation, the anti-His surface was regenerated by injecting a single pulse of 10 mM glycine (pH 1.5) for 60 s at a flow rate of 30 μl/min.

Enzyme-linked immunoabsorption assay (ELISA). Briefly, purified His-tagged Env proteins were captured onto preblocked Ni-NTA 96-well plates (Qiagen) via their tags by incubation for 2 h at 0.5 μg/ml in Tris-buffered saline (TBS) containing 5% fetal bovine serum (FBS). The test MAbs or related reagents were then added for 1 h in the same buffer. Bound MAbs were detected using an appropriate horseradish peroxidase (HRP)-conjugated secondary antibody and the 3,3′,5,5′-tetramethylbenzidine (TMB) substrate system with an optical density endpoint at 450 nm (Bio-Rad). The 50% binding values (50% effective concentrations [EC_{50}s]) for MAb binding were calculated by plotting the nonlinear regression curves using Prism software, version 5.0.

Neutralization assay. The neutralization sensitivity of Env-pseudotyped viruses was determined using the Tzm-bl cell assay as described previously (18, 28). The test viruses are based on the full-length *env* genes. All assays were performed in duplicate. Virus infectivity in the absence of a test MAb was defined as 100%. The MAb concentrations reducing infectivity by 50% (IC_{50}s) were calculated from nonlinear regression fits of a sigmoid function to the normalized inhibition data by the use of Prism software, version 5.0.

Correlations between the neutralization assay IC_{50}s and the ELISA EC_{50}s were investigated using the nonparametric Spearman's rank correlation test and the same software program.

Differential scanning calorimetry (DSC). The thermal denaturation of purified Env proteins, previously dialyzed into phosphate-buffered saline (PBS) and added to the test cell at a concentration of 100 to 300 μg/ml, was probed using a MicroCal VP-Capillary DSC calorimeter (Malvern Instruments) as described previously (18). The scan rate for the temperature increase was 90°C/h. Buffer correction, normalization, and baseline subtraction procedures were applied before the data were analyzed using Origin 7.0 software. The resulting data were fitted using a non-two-state model, as the asymmetry of some of the thermal denaturation peaks suggested that unfolding intermediates were present.

Glycan profiling of Env proteins. N-linked glycosylation profiles of purified Env proteins were determined by hydrophilic interaction liquid chromatography-ultraperformance liquid chromatography (HILIC-UPLC) as previously described (39). Briefly, purified Env proteins (10 μg) were fractionated by SDS-PAGE under reducing or nonreducing conditions. The gels were stained with Coomassie blue. Bands corresponding to the gp140, gp120, or gp41$_{ECTO}$ species were excised from the gels, which were washed with acetonitrile and then washed with water; this procedure was repeated five times. N-linked glycans were then released by addition of protein *N*-glycosidase F (PNGase F) at 5,000 U/ml and incubation at 37°C for 16 h, according to the manufacturer's instructions (New England BioLabs [NEB]). Released glycans were eluted from the gel bands by extensive washing with water, dried using a SpeedVac concentrator, labeled with 2-aminobenzoic acid (2-AA), and then purified as previously described (39). Fluorescently labeled glycans were resolved by HILIC-UPLC using a Acquity BEH amide column (2.1 mm by 10 mm) as described previously (39). Data processing was performed using Empower 3 software. The percentage abundance of oligomannose-type glycans was calculated by integration of the relevant peak areas before and after endoglycosidase H digestion, following normalization.

Hydrogen/deuterium exchange mass spectrometry (HDX-MS). The 92UG037.8 and CZA97.012 SOSIP.664-His trimers were purified by bNAb PGT145 and PGT151 columns, respectively, whereas the gp140$_{UNC}$-Fd-His versions were purified by Ni-NTA columns. For all four proteins, SEC was carried out as described above. After SEC purification, the proteins were concentrated to ~0.5 mg/ml using Vivaspin filters (100-kDa molecular-weight cutoff [MWCO]; GE Healthcare). The HDX methodology, including peptide identification, was performed as described previously (48). Deuterium exchange was initiated by 10-fold dilution into deuterated PBS buffer at 23°C. Samples were quenched after 3 s, 1 min, 30 min, and 20 h by mixing 1:1 with ice-cold acidification buffer (0.2% formic acid, 200 mM Tris 2-carboxyethyl-phosphine [final pH 2.5]). Samples were immediately frozen in liquid nitrogen and stored at −80°C. An internal PPPI peptide at a concentration of 0.5 μg/ml was included to ensure that deuterium labeling conditions were consistent for each sample (49). Fully deuterated control samples were prepared by denaturing gp140 samples in 4 M guanidinium hydrochloride (Gnd-HCl)–20 mM DTT at 85°C for 30 min, followed by a 10-fold dilution into deuterated PBS and incubation at 60°C for 2 h.

Liquid chromatography coupled to mass spectrometry (LC/MS) was performed by manually loading samples onto a Waters HDX manager coupled with a Waters Synapt G2Si mass spectrometer. The samples were passed through a pepsin column (2.1 by 50 mm) (kept at 0.5°C) at a flow rate of 150 μl/min and subsequently loaded onto a Waters Vanguard C$_{18}$ guard column (2.1 by 5 mm). A gradient of 5 to 50% solvent B (solvent A consisted of 0.1% formic acid, 0.04% trifluoroacetic acid, and 2% acetonitrile; solvent B consisted of 99.9% acetonitrile and 0.1% formic acid) was used to resolve the peptides over a BEH C$_{18}$ column (1 by 100 mm) (Waters) at 40 μl/min, which was also kept at 0.5°C. After each injection, the pepsin column (50), the trap, and the analytical columns (51) were extensively washed to minimize sample carryover. The resulting data were analyzed using HX-Express v2 (52). The percent exchange is reported for each peptide relative to zero and fully deuterated standards. Error bars reflect the standard deviations between duplicate measurements. The data from the 92UG037.8 monomeric gp120 protein and the BG505 SOSIP.664 trimer were published previously (41, 48).

Analysis of disulfide bond formation in Env proteins. Disulfide bond patterns in CZA97012 gp140 glycoproteins were determined by liquid chromatography coupled to tandem mass spectrometry (LC/MS/MS) analysis of tryptic digestion products of alkylated and deglycosylated gp140 samples, as described previously (53, 54). In brief, ~50 μg of protein was alkylated with 4-vinylpyridine to cap free cysteine residues prior to deglycosylation. Samples were subsequently deglycosylated with PNGase F at 37°C for a week. Fully deglycosylated, alkylated samples were digested overnight with trypsin and were subsequently analyzed using a linear ion trap (LTQ) Orbitrap Velos Pro (Thermo Scientific, San Jose, CA) mass spectrometer coupled to an Acquity ultraperformance liquid chromatography (UPLC) system (Waters, Milford, MA). Chromatogra-

phy was performed using mobile phases consisting of solvent A (99.9% deionized H_2O plus 0.1% formic acid) and solvent B (99.9% CH_3CN plus 0.1% formic acid) and a 3% to 40% solvent B gradient in 50 min at 5 μl/min through a C_{18} PepMap 300 column (300-μm inner diameter [i.d.] by 15 cm and 300-Å pore size; Thermo Scientific Dionex, Sunnyvale, CA). Mass spectrometric (MS) analysis was performed in a data-dependent acquisition mode consisting of one full MS scan followed by three MS/MS events of the top three most intense ions. Each ion was sequentially and dynamically selected for collision-induced dissociation (CID), electron transfer dissociation (ETD), and CID of the charge-reduced precursor in the previous ETD event in the LTQ mass spectrometer. The presence of each disulfide-bonded peptide was determined using high-resolution MS, with 10 ppm as the maximum mass error, and confirmed by manual assignment of the corresponding MS/MS data, as described previously (54, 55).

Negative-stain electron microscopy. Env proteins were prepared for negative-stain electron microscopy (EM) analysis as previously described (18, 28). Briefly, a 3-μl aliquot containing 0.01 to 0.05 mg/ml of Env protein (as determined by UV spectroscopy at 280 nm using a theoretical extinction coefficient based on the peptide sequence alone) was applied for 5 s onto a carbon-coated 400-mesh Cu grid that had been glow discharged at 20 mA for 30 s and then negatively stained with 2% (wt/vol) uranyl formate for 60 s. Grids were screened to assess stain quality and particle distribution. The sample concentration was adjusted, and the grids were remade until the particle overlap on the grid surface had been minimized. Data were collected either on an FEI Tecnai T12 electron microscope operating at 120 keV, with an electron dose of ~25 $e^-/Å^2$ and a magnification of ×52,000 that resulted in a pixel size of 2.05 Å on the specimen plane, or on an FEI Talos electron microscope operating at 200 keV, with an electron dose of ~25 $e^-/Å^2$ and a magnification of ×73,000 that resulted in a pixel size of 1.98 Å on the specimen plane. Images were acquired with a Tietz TemCam-F416 CMOS camera (FEI Tecnai T12) or a FEI Ceta 16M camera (FEI Talos) using a nominal defocus range of 1,000 to 1,500 nm.

Data processing methods were adapted from those used previously (28). The resulting two-dimensional (2D) class averages were visually inspected, and discernible aggregates, dimers, and monomers (based on relative mass/size) were removed from an additional round of 2D classification. The updated classes were segregated into one of three structural groups labeled closed, open, or nonnative as described previously (28). The amount of native-like particles was defined as the sum of closed and open particles.

RESULTS

Design, expression, and biochemical properties of gp140 proteins. The various gp140 proteins shown in Fig. 1 were based on the 92UG037.8 (clade A) and CZA97.012 (clade C) *env* gene sequences. The design of the standard uncleaved gp140 proteins, here designated gp140$_{UNC}$-Fd-His, is identical to the designs of the gp140 proteins described in multiple publications (2, 42, 43). The natural REKR cleavage site between gp120 and gp41$_{ECTO}$ is present in both these gp140 constructs but is used to a negligible extent (see below). The Foldon domain and a His tag are present at the gp41$_{ECTO}$ C termini, again as described previously (2, 42, 43). Variants of these proteins containing additional modifications are described below. The SOSIP.664-His versions of the 92UG037.8 and CZA97.012 proteins were made by introducing an optimized cleavage site (RRRRRR), the SOS disulfide bond to link the gp120 and gp41$_{ECTO}$ subunits, and the I559P substitution in gp41$_{ECTO}$, all of which have been described elsewhere (18). In addition, the 92UG037.8 and CZA97.012 SOSIP.664-His gp140s contain one substitution and two other substitutions in gp41$_{ECTO}$, I535M and L535M plus Q567K, respectively, that modestly improve trimer formation (44). The SOSIP trimers also include a C-terminal His
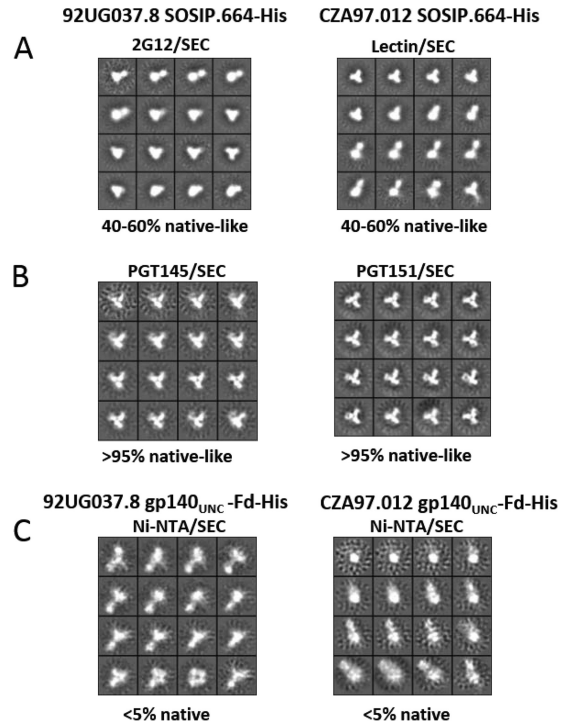

FIG 2 Negative-stain EM reference-free 2D class averages of 92UG037.8 and CZA97.012 SOSIP.664-His and gp140$_{UNC}$-Fd-His proteins purified by different methods. (A) 92UG037.8 SOSIP.664-His trimers purified by 2G12/SEC and CZA97.012 SOSIP.664-His trimers purified by GNA-lectin/SEC; (B) 92UG037.8 SOSIP.664-His trimers purified by PGT145/SEC and CZA97.012 SOSIP.664-His trimers purified by PGT151/SEC; (C) 92UG037.8 and CZA97.012 gp140$_{UNC}$-Fd-His proteins purified by Ni-NTA/SEC. The percentage of native-like trimers is listed below each set of class averages. Any discernible aggregates, dimers, and monomers (based on relative mass/size) are not included in the class averages or the calculations of the percentage of native-like trimers.

tag immediately after residue 664 to allow a comparison with the uncleaved gp140$_{UNC}$-Fd-His proteins in antigenicity assays such as SPR assay and ELISA (Fig. 1).

The above four Env proteins were produced in 293F cells by transient transfection using 293Fectin. For expression of the SOSIP.664-His proteins, furin was cotransfected to facilitate gp140 cleavage (18). However, furin was not cotransfected with the gp140$_{UNC}$-Fd-His proteins to ensure comparability with earlier reports on the properties of these proteins (2, 42, 43). The 92UG037.8 and CZA97.012 gp140$_{UNC}$-Fd-His gp140s were purified via their His tags using Ni-NTA columns as described previously (2, 42), followed by SEC (Ni-NTA/SEC) to isolate the trimer fraction (2, 42). We used this procedure to maximize comparability between our data and what has been reported for the same proteins (2, 4, 5, 42). We conducted pilot experiments to assess how best to purify the newly generated 92UG037.8 and CZA97.012 SOSIP.664-His trimers, in a form that was as fully native-like as possible. Initial antigenicity studies on unpurified transfection supernatants suggested that a 2G12 bNAb column and a GNA-lectin column, again followed by SEC, would be suitable for making initial preparations of 92UG037.8 and CZA97.012 SOSIP.664-His trimers, respectively. The resulting purified trimers were studied by negative-stain EM and found to contain mixtures of native-like and nonnative trimers in approximately equal amounts (Fig. 2A).
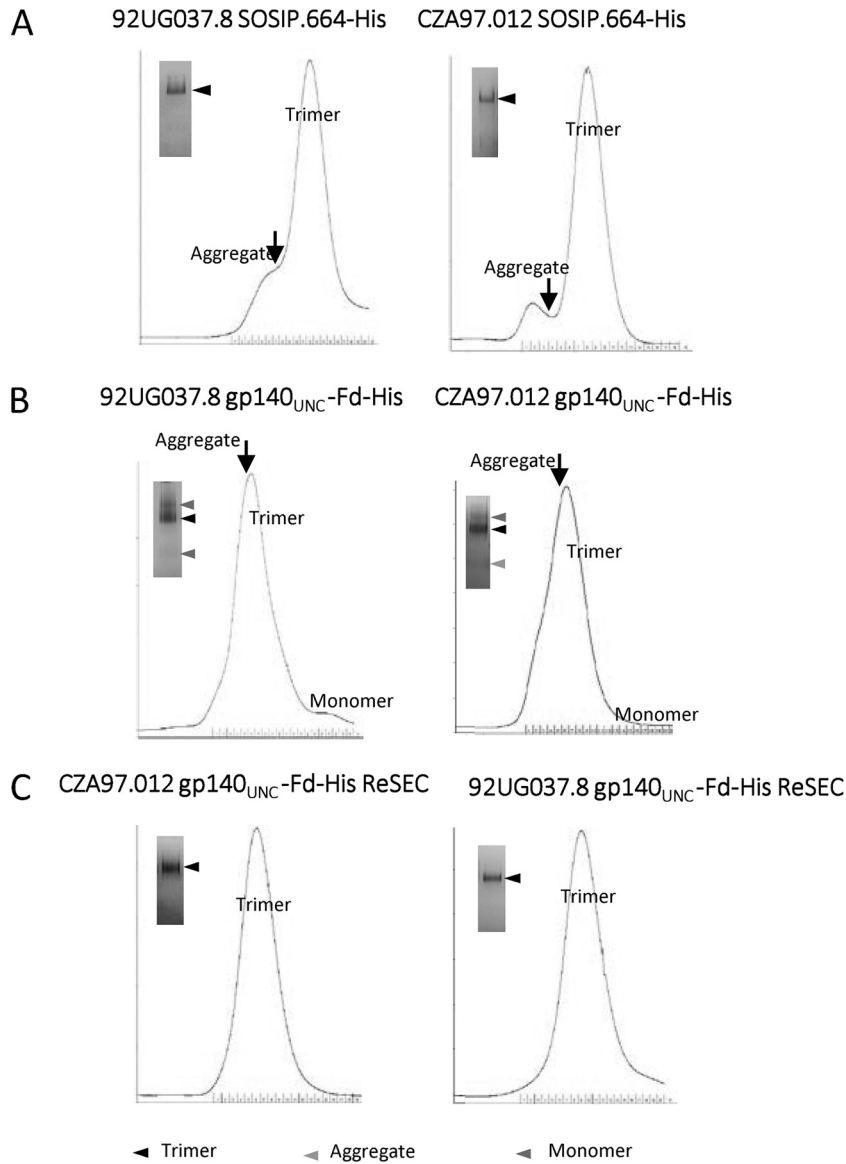
FIG 3 SEC profiles of SOSIP.664-His and gp140_UNC-Fd-His proteins. (A) PGT145-purified 92UG037.8 and PGT151-purified CZA97.012 SOSIP.664-His proteins; (B) Ni-NTA-purified 92UG037.8 and CZA97.012 gp140_UNC-Fd-His proteins. In panel B, the arrows show when collection of the trimer fractions was initiated. (C) The trimer fractions shown in panel B were pooled and reanalyzed by SEC (ReSEC). In each panel, the x axis shows the fractions collected over time and the y axis shows absorbance at 280 nm. In each panel, the inset shows a BN-polyacrylamide gel with the most prominent bands indicated.

However, pilot-scale antigenicity assessments showed that the 92UG037.8 and CZA97.012 SOSIP.664-His trimers reacted well with the trimer-specific (i.e., quaternary structure-dependent) bNAbs PGT145 and PGT151, respectively (data not shown). On the basis of our earlier use of PGT145 columns, we judged that we could purify fully native-like SOSIP.664-His trimers by positive selection followed by SEC (28, 39). The Ni-NTA column is not appropriate for purifying either SOSIP.664-His trimer, because as noted previously, this method is not conformationally selective and yields mixtures of native-like and nonnative trimers (39).

When EM was used to visualize the PGT145/SEC-purified 92UG037.8 SOSIP.664-His trimers and PGT151/SEC-purified CZA97.012 SOSIP.664-His trimers, essentially all were found to be native-like, with >90% in the fully closed conformation

(Fig. 2B). The yield of trimers purified by positive selection was reduced by ~2.5-fold compared to the lectin/SEC and 2G12/SEC methods, reflecting the elimination of the nonnative trimer components. Although SEC is not strictly necessary to purify trimers that have already been isolated via the trimer-specific bNAb columns, we continued to routinely use this secondary technique to allow comparability with the uncleaved 92UG037.8 and CZA97.012 gp140s, for which the SEC stage was essential.

SEC profiles of the PGT145- or PGT151-purified SOSIP.664-His gp140 preparations showed sharp, trimer-containing peaks. The very few protein aggregates (<5%) present were well separated from the trimer fractions (Fig. 3A). The deletion of the membrane-proximal external region (MPER) and the occlusion of other hydrophobic areas of gp41_ECTO by the overlying gp120
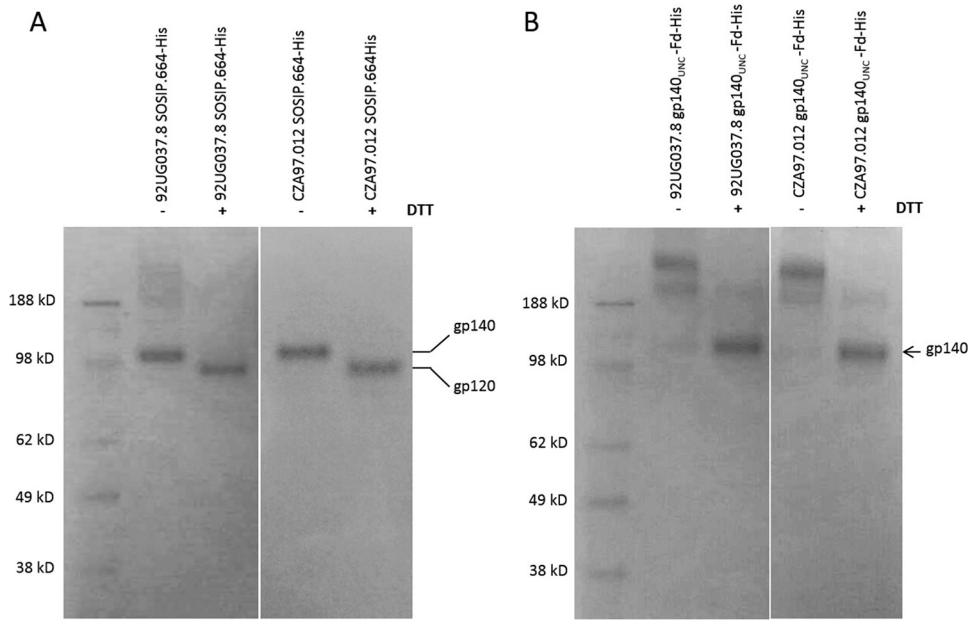
FIG 4 SDS-PAGE analysis of SOSIP.664-His and gp140$_{UNC}$-Fd-His proteins. (A and B) Reducing gels (i.e., with DTT [+ DTT]) versus nonreducing gels of PGT145/SEC-purified 92UG037.8 and PGT151/SEC-purified CZA97.012 SOSIP.664-His trimers (A) and Ni-NTA-purified 92UG037.8 and CZA97.012 gp140$_{UNC}$-Fd-His proteins (B). The positions of gp120 and gp140 bands are indicated by the black lines or black arrow to the right of the gels. The positions of molecular mass markers (in kilodaltons) are indicated to the left of the gels.

subunits accounts for why SOSIP.664 proteins aggregate only minimally (1, 8, 45, 56). In contrast, the SEC profiles of the Ni-NTA-purified gp140$_{UNC}$-Fd-His proteins revealed a quantitatively dominant single peak that contained high-molecular-weight (MW) protein aggregates, followed by trimers, with a small amount (1 to 3% of the total) of later-eluting gp140 monomers also present (Fig. 3B, graphs). The overlap with the aggregated material complicates purification of uncleaved trimers, which accordingly often contain significant amounts of aggregates (2, 4, 42, 43). Some of these forms represent disulfide cross-linked gp140 oligomers (see below), while others probably arise via noncovalent associations involving the membrane-proximal external region (MPER) and other hydrophobic areas of gp41$_{ECTO}$. Nonetheless, by adopting a conservative fraction collection strategy that favored purity over yield (see arrows in Fig. 3B), we were able to isolate gp140$_{UNC}$-Fd-His proteins that migrated as a single peak when they were reanalyzed by SEC (Fig. 3C, graphs) and ran as a single band on a BN-polyacrylamide gel (Fig. 3C, insets). Negative-stain EM images of these proteins were taken (Fig. 2C) and are described below.

Reducing versus nonreducing SDS-polyacrylamide gels were then used to further study the gp140 proteins that were purified by affinity columns (PGT145 or PGT151) and then SEC (Fig. 4A). The SOSIP.664-His trimers ran as single bands and were both fully cleaved between gp120 and gp41$_{ECTO}$, as indicated by the conversion of the gp140 band into gp120 in the presence of DTT. In contrast, the two gp140$_{UNC}$-Fd-His proteins were completely uncleaved (i.e., no conversion of gp140 to gp120 when DTT was present). Higher-MW aggregates were clearly visible in the uncleaved gp140 preparations when the gels were run under nonreducing conditions, and their sensitivity to DTT implies that they are the products of gp140 cross-linking via intermolecular disulfide bonds (Fig. 4B). Such disulfide bond-linked aggregates are

routinely seen in uncleaved gp140 preparations (32, 36, 57). How they arise is discussed further below.

Protease sensitivity of SOSIP.664-His trimers and gp140$_{UNC}$-Fd-His proteins. The protease sensitivity of the purified gp140 proteins was studied by incubating them with various concentrations of trypsin, chymotrypsin, or proteinase K for 1 h at 37°C followed by reducing SDS-PAGE (Fig. 5). The two SOSIP.664-His trimers were unaffected by trypsin and chymotrypsin under these conditions, but the 92UG037.8 trimers were partly and nearly completely degraded at proteinase K concentrations of 0.1 and 1 μg/ml, respectively, and CZA97.012 trimers were completely degraded at a proteinase K concentration of 1 μg/ml. In contrast, both of the gp140$_{UNC}$-Fd-His proteins were almost completely digested by each of the three proteases at 1 μg/ml and were detectably damaged by 10-fold-lower concentrations. Overall, the SOSIP.664-His trimers are more than 10-fold more resistant to proteases, which is consistent with earlier reports (19, 30).

Negative-stain EM imaging of optimally purified SOSIP.664-His trimers and gp140$_{UNC}$-Fd-His proteins. As noted above, we first obtained EM images of the 92UG037.8 and CZA97.012 SOSIP.664-His trimers to guide the design of the optimal purification strategy for these proteins (Fig. 2A). When the 92UG037.8 and CZA97.012 SOSIP.664-His trimers were purified by PGT145/SEC and PGT151/SEC, respectively, and analyzed by EM, these trimers are indistinguishable from their well-characterized 2G12/SEC-purified BG505 SOSIP.664 counterparts, in that all three trimer populations are almost completely native-like and dominated by fully symmetric, trilobed structures (Fig. 2B). Moreover, these trimers are predominantly in the fully closed conformation (>90% for both 92UG037.8 and CZA97.012), again mirroring the appearance of the BG505 trimers (~100% closed). The remaining trimer structures are still native-like but partially open, akin to what we have described as a major subpopulation
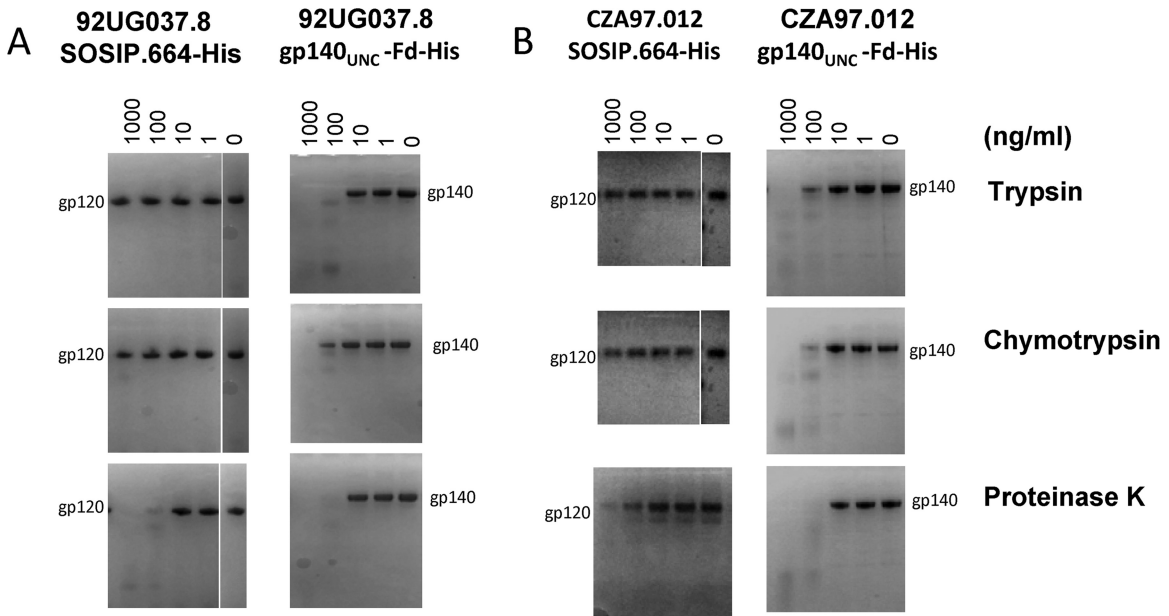
FIG 5 Protease sensitivity of SOSIP.664-His trimers and gp140_UNC-Fd-His proteins. (A and B) 92UG037.8 (A) and CZA97.012 (B) proteins were incubated with the indicated concentrations (in nanograms per milliliter) of trypsin, chymotrypsin, or proteinase K for 1 h at 37°C and analyzed by reducing SDS-PAGE. The 92UG037.8 and CZA97.012 SOSIP.664-His trimers were purified by the PGT145/SEC and PGT151/SEC methods, respectively, and the two gp140_UNC-Fd-His proteins were purified via Ni-NTA/SEC. In panels A and B, the 0-concentration lanes of the trypsin and chymotrypsin gels are duplicate depictions of the same control samples, as they are common to both of the protease titration experiments that were performed simultaneously and analyzed on the same gel.

in B41 SOSIP.664 trimer preparations (28). Versions of the two new SOSIP.664 trimers that lack the His tag are indistinguishable from their tagged counterparts (data not shown).

In marked contrast, native-like trimer structures were very rarely seen (<5% frequency) in each of the two Ni-NTA/SEC-purified gp140_UNC-Fd-His preparations (Fig. 2C). Instead, the predominant images depict splayed-out structures that represent decayed or never-formed trimers held together by the uncleaved peptide linking gp120 to gp41_ECTO. The images are highly similar

to what has been found with several other uncleaved gp140s of the standard (i.e., nonlinker) design, based on various genotypes and containing or lacking a Foldon domain (7, 16, 19, 30, 39).

Antigenic structures of SOSIP.664-His and gp140_UNC-Fd-His proteins assessed by SPR. We used SPR to compare the antigenicity of the Ni-NTA/SEC-purified 92UG037.8 and CZA97.012 gp140_UNC-Fd-His proteins with the corresponding fully native-like SOSIP.664-His trimers (i.e., PGT145/SEC purified for 92UG037.8, PGT151/SEC purified for CZA97.012) (Fig. 6A and
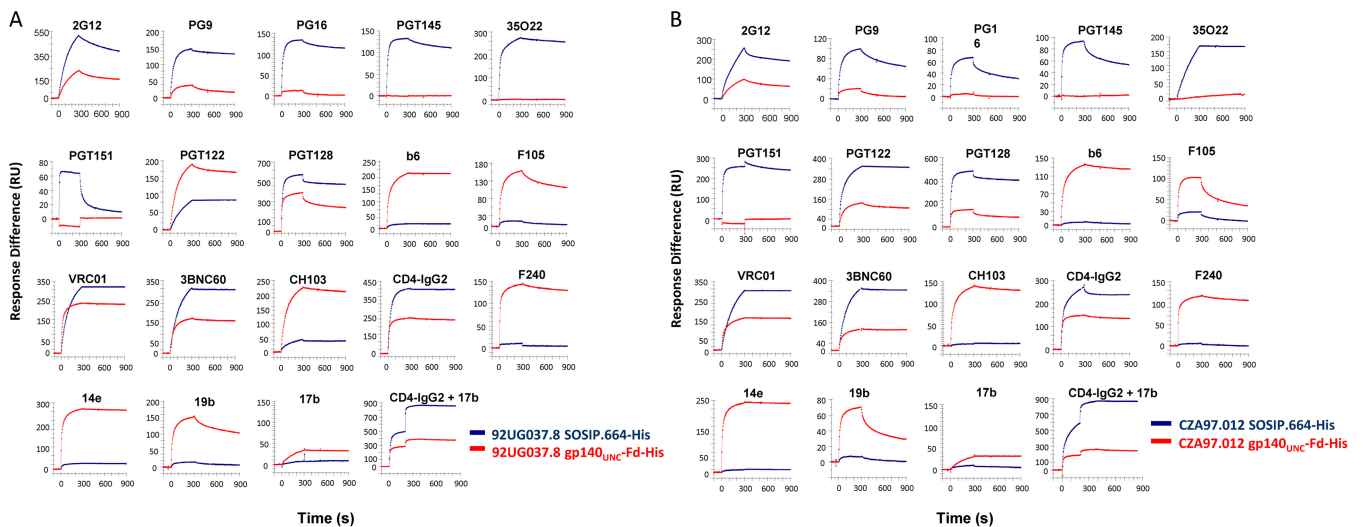
FIG 6 SPR analyses of SOSIP.664-His trimers and gp140_UNC-Fd-His proteins. Association and dissociation profiles for the indicated MAbs are shown. CD4-IgG2 and all MAbs other than 2G12 at 500 nM flowed over His tag-immobilized Env proteins that were present on the chips in equivalent amounts (~5% standard deviation [SD]). The 2G12 MAb was injected at 62 nM (see Materials and Methods). (A) 92UG037.8 proteins; (B) CZA97.012 proteins. Note that the y-axis scales differ among the plots. The Env proteins were purified as described in the legend to Fig. 5.

TABLE 1 MAb neutralization and Env-binding ELISA titers

| Epitope | Antibody[a] | 92UG037.8[b] | | | CZA97.012[b] | | |
| | | Neutralization IC$_{50}$ (ng/ml) | ELISA binding EC$_{50}$ (ng/ml) | | Neutralization IC$_{50}$ (ng/ml) | ELISA binding EC$_{50}$ (ng/ml) | |
			SOSIP.664-His trimer	gp140$_{UNC}$-Fd-His		SOSIP.664-His trimer	gp140$_{UNC}$-Fd-His
CD4bs	CD4-IgG2	1,900	5,000	65	3,900	5,000	200
	VRC01	230	350	50	900	6,500	300
	3BNC60	40	1,100	180	400	6,000	5,000
	CH103	12,300	>10,000	550	>30,000	>10,000	300
	b12	>30,000	>10,000	5,000	>30,000	>10,000	5,000
	b6	>30,000	>10,000	400	>30,000	>10,000	110
	F105	>30,000	>10,000	450	>30,000	>10,000	5,000
V1/V2-glycan	PG9	160	3,600	>10,000	>30,000	>10,000	>10,000
	PG16	30	550	>10,000	>30,000	>10,000	>10,000
	PGT145	3,150	1,370	>10,000	4,160	>10,000	>10,000
V3-glycan	PGT122	1,200	4,000	550	40	115	800
	PGT128	50	218	25	80	100	500
OD-glycan	2G12	>30,000	2,910	5,000	>30,000	>10,000	>10,000
	PGT135	>30,000	>10,000	9,000	>30,000	>10,000	>10,000
gp120-gp41 interface	PGT151	>30,000	>10,000	>10,000	170	100	>10,000
	35022	30,000[c]	55	>10,000	>30,000	1,000	>10,000
	8ANC195	6,700	5,000	>10,000	>30,000	>10,000	>10,000
MPER	2F5	3,024[d]	NA	>10,000	>30,000[d]	NA	>10,000
	4E10	8,840[d]	NA	>10,000	4,700[d]	NA	>10,000
V3	14e	>30,000	>10,000	150	>30,000	>10,000	300
	19b	>30,000	>10,000	600	>30,000	>10,000	>10,000
	39F	>30,000	>10,000	520	>30,000	>10,000	1,000
CD4i	17b	>30,000	>10,000	9,000	>30,000	>10,000	1,600
Cluster I (gp41)	F240	>30,000	>10,000	25	>30,000	>10,000	20

[a] The test MAbs are grouped by epitope cluster.

[b] The values shown in the table are 50% neutralization titers (IC$_{50}$ [in nanograms/milliliter]) derived from Env-pseudotyped virus-based assays in Tzm-bl cells and midpoint binding titers (EC$_{50}$ [in nanograms/milliliter]) from His tag ELISAs using the SOSIP.664-His and gp140$_{UNC}$-Fd-His Env proteins. The > symbol in front of values indicates that endpoints were not achieved at MAb concentrations of 30,000 ng/ml in the neutralization assay or 10,000 ng/ml in the ELISA. NA, not applicable (SOSIP.664 trimers do not express epitopes for bNAbs against the MPER).

[c] For bNAb 35O22 versus the 92UG037.8 virus, an IC$_{50}$ could not be determined precisely because the extent of neutralization reached a plateau value at ~50% (see the text).

[d] Values for neutralization by MAbs 2F5 and 4E10 were derived from reference 87.

B). In this SPR method, the Env proteins are first captured onto CM5 chips via their His tags, which are recognized by a covalently bound anti-His MAb. Anti-Env MAbs are then allowed to flow over the captured Env proteins, and the MAb-Env association and dissociation phases are recorded (26). In all experiments, equivalent amounts of different Env proteins were confirmed to be present on the SPR chips, allowing their reactivity with test MAbs to be compared directly. In contrast, the more commonly used SPR method in which the Env protein flows in a solution over chip-immobilized MAbs does not allow such comparisons, and in addition, this method often detects the MAb binding of only a small subset of the input proteins (2, 5, 26).

Several bNAbs and non-NAbs against the CD4 binding site (CD4bs), and the CD4-IgG2 protein, were used to probe the accessibility of this region of the 92UG037.8 Env proteins (Fig. 6A). The VRC01 and 3BNC60 bNAbs and the CD4-IgG2 protein each bound to both Env proteins, but the maximum signals were 1.5- to 2-fold greater for SOSIP.664-His than for gp140$_{UNC}$-Fd-His. In

contrast, the b6 and F105 non-NAbs to CD4bs-associated epitopes reacted only minimally with the SOSIP.664-His trimer, but they reacted strongly with the gp140$_{UNC}$-Fd-His protein. CH103, a CD4bs MAb, which had some breadth of reactivity overall but was only weakly neutralizing and nonneutralizing for the 92UG037.8 and CZA97.012 Env-pseudotyped viruses (IC$_{50}$s, 12.3 and >30 μg/ml, respectively; Table 1), behaved similarly to b6 and F105 when tested against the two 92UG037.8 Env proteins (and also the two CZA97.012 proteins) (Fig. 6A and B). The pattern of reactivity with the CD4bs suggests that the quaternary structural constraints on the accessibility of non-bNAb epitopes are much greater within the SOSIP.664-His trimers, which instead present the bNAb epitopes better than the gp140$_{UNC}$-Fd proteins do. The non-NAb 17b to a CD4-induced (CD4i) epitope bound weakly to the gp140$_{UNC}$-Fd-His protein in the absence of soluble CD4 (sCD4), but its epitope was induced by prior CD4-IgG2 binding (RU values of 29 ± 0.50 versus 110 ± 1.7 [mean ± standard error of the mean{SEM}], with and without CD4-IgG2, respectively).

However, the extent to which CD4-IgG2 induced the 17b epitope was much greater on the SOSIP.664-His trimer, and the epitope was not accessible before CD4-IgG2 addition (RU values of 8.0 ± 2 versus 370 ± 7.1 with and without CD4-IgG2, respectively). The V3-targeting non-NAbs 14e and 19b and the gp41 cluster I non-NAb F240 all bound strongly to the gp140$_{UNC}$-Fd-His protein, but negligibly to the SOSIP.664-His trimer. The PGT122 bNAb against a glycan-dependent V3 epitope reacted better with the gp140$_{UNC}$-Fd-His protein, but the converse applied to the PGT128 bNAb against a similar V3-glycan epitope. The 2G12 bNAb reacted more strongly with the SOSIP.664-His trimer by approximately twofold, again judged by the maximum level of binding. The influence of appropriate trimerization on epitope exposure was dramatically illustrated by the antigenicity profiles for the trimer-specific or trimer-influenced bNAbs PG9, PG16, PGT145, PGT151, and 35O22, which bound only, or to vastly greater extents, to the SOSIP.664-His trimers. It is noteworthy that a very rapid off-rate was observed for PGT151 (see below). Thus, the 92UG037.8 SOSIP.664-His proteins have all the hallmarks of native-like trimers, while their uncleaved gp140$_{UNC}$-Fd-His counterparts have none of the hallmarks (Fig. 6A). The SPR antigenicity profiles are therefore entirely concordant with the EM images of the same 92UG037.8 Env proteins (Fig. 2B and C).

A very similar SPR data set was obtained using the two CZA97.012 Env proteins, leading to the same conclusion that the SOSIP.664-His trimers are native-like structures that display quaternary epitopes (i.e., PG9, PG16, PGT145, 35O22, PGT151). The PGT151 bNAb against one such epitope at the gp120-gp41 interface bound with high affinity, but bNAbs PG9, PG16, and PGT145 to trimer apex epitopes had rapid dissociation rates (see below). In contrast, the gp140$_{UNC}$-Fd-His proteins lack these critical properties (Fig. 6B). Again, the antigenicity profiles are consistent with the respective EM images (Fig. 2B and C). Unlike 92UG037.8, CZA97.012 gp120 lacks a glycan at residue 295. This glycan site is generally considered to be one of the principal components of the 2G12 epitope (58–63). Nonetheless, we observed that 2G12 could still bind efficiently to the CZA97.012 Env proteins in the SPR assay (Fig. 6B). We also found that, unexpectedly, the 2G12 affinity column could be used to purify the CZA97.012 SOSIP.664-His proteins, an observation similar to ones made with other trimers based on different clade C env genes (64). The explanation may be rooted in promiscuous glycan recognition, where the lack of a glycan from certain bNAb epitopes, including 2G12, can be compensated for by the presence of another glycan (46, 47). Here, it is notable that any secondary, lower-affinity glycan-binding site for 2G12 on SOSIP.664 trimers may be absent from the gp140$_{UNC}$-Fd-His proteins, which have non-native glycan profiles (see below).

In contrast to the results with the 92UG037.8 proteins, the PGT122 bNAb was more reactive with its V3-glycan epitope on the CZA97.012 SOSIP.664-His trimer than on the gp140$_{UNC}$-Fd-His gp140 (Fig. 6B). However, as with the 92UG037.8 proteins, PGT128 bound better to its V3-glycan epitope on the CZA97.012 SOSIP.664-His trimer, compared to the corresponding uncleaved gp140 (Fig. 6B). The lower reactivity of PGT122 with the 92UG037.8 SOSIP.664-His trimers than the corresponding gp140$_{UNC}$-Fd-His proteins (also seen in ELISA; Table 1) may relate to genotype-dependent glycosylation differences. In general, uncleaved gp140s have a higher content of processed glycans than native-like trimers (see below), and the PGT122 epitope, but not

the PGT128 epitope, includes this type of glycan in at least some sequence contexts (65) The induction of the 17b epitope by CD4-IgG2 was, again, much greater for the SOSIP.664-His trimer (RU values of 9.5 ± 1.5 versus 280 ± 5.5 with and without CD4-IgG2, respectively) than for the gp140$_{UNC}$-Fd-His protein (RU values of 34 ± 0.50 versus 76 ± 1.3). For the CZA97.012 SOSIP.664-His trimer, the off-rate for PGT145 was rapid, but for PGT151, it was more moderate, the converse of what was seen with its 92UG037.8 counterpart. The pattern of reactivity of these two exquisitely trimer-specific bNAbs is consistent with our earlier anecdotal observations that the PGT145 bNAb column could be used to purify the 92UG037.8, but not the CZA97.012, SOSIP.664-His trimers and vice versa for the PGT151 column.

Neutralization of Env-pseudotyped viruses compared to antigenicity of Env proteins in ELISAs. To assess whether there are antigenic similarities between the 92UG037.8 and CZA97.012 Env proteins and the native Env spike on the corresponding virus particles, we first used a panel of bNAbs and non-NAbs as probes in a Tzm-bl cell-based neutralization assay that used Env-pseudotyped viruses based on the full-length gp120 and gp41 sequences. We then tested the same antibodies in a His tag capture ELISA to measure Env binding and derive EC$_{50}$s (Fig. 7 and Table 1). We used an ELISA for this purpose because of the greater ease with which a large panel of MAbs can be tested, compared to the SPR assay, while being aware of the limitations associated with this method (18, 28). The test antibodies were again chosen to span a range of epitopes on the trimer surface. The VRC01 and 3BNC60 bNAbs and the CD4-IgG2 molecule, which all target the CD4bs, neutralized both Env-pseudotyped viruses, whereas CH103 weakly neutralized only 92UG037.8 and b12 was ineffective against both viruses (Table 1). As expected, the non-NAbs to CD4bs (b6 and F105), CD4i (17b), V3 (14e, 19b, and 39F) and gp41 cluster I (F240) epitopes all failed to neutralize either the 92UG037.8 or CZA97.012 virus (Table 1). The V3-glycan-targeting bNAbs PGT122 and PGT128 neutralized both viruses, but the outer-domain glycan-targeting bNAbs 2G12 and PGT135 neutralized neither. Among the quaternary structure-dependent bNAbs to epitopes at the trimer apex, PG9, PG16, and PGT145 neutralized the 92UG037.8 virus, but only PGT145 was effective against the CZA97.012 virus. Of the three bNAbs against quaternary epitopes at the gp120-gp41 interface, PGT151, 35O22, and 8ANC195, only 8ANC195 was able to neutralize 92UG037.8 effectively, and only PGT151 was active against CZA97.012.

For each Env protein, the overall set of ELISA EC$_{50}$s was then compared with the IC$_{50}$s for neutralization of the corresponding Env-pseudotyped viruses, essentially as described previously (18, 28) (Fig. 7A). For the SOSIP.664-His trimers, the resulting Spearman's correlation coefficients, r, were 0.70 (95% confidence interval, 0.39 to 0.87; P < 0.0003) and 0.83 (95% confidence interval, 0.63 to 0.93; P < 0.0001) for the 92UG037.8 and CZA97.012 SOSIP.664-His trimers, respectively, i.e., the neutralization of the corresponding Env-pseudotyped viruses correlated well with the binding to the SOSIP.664-His trimer. In marked contrast, when similar comparisons were conducted using the ELISA binding EC$_{50}$s for the two gp140$_{UNC}$-Fd-His Env proteins, there were no correlations with the neutralization sensitivities of the corresponding Env-pseudotyped viruses (r = 0.06 and 0.16 and P = 0.70 and 0.47 for 92UG037.8 and CZA97.012, respectively [Fig. 7B]). We conclude that the 92UG037.8 and CZA97.012 SOSIP.664-His proteins are good antigenic mimics of the func-
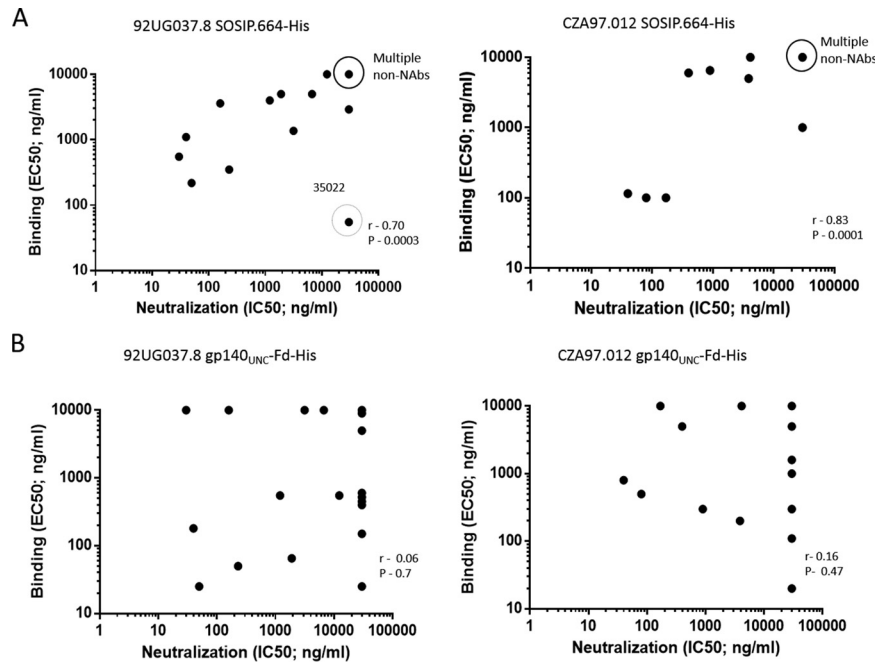
FIG 7 Correlation between antigenicity of SOSIP.664 trimers and neutralization of Env-pseudotyped viruses. The plots for 92UG037.8 and CZA97.012 compare EC_{50}s for MAb binding derived from His tag capture ELISAs with IC_{50}s derived from TZM-bl cell neutralization assays using the same MAbs and the corresponding Env-pseudotyped viruses. Data on the MPER-specific bNAbs 2F5 and 4E10 were not included in these analyses, as these epitopes are not present on SOSIP.664-His trimers. (A) PGT145/SEC- or PGT151/SEC-purified SOSIP.664-His trimers; (B) Ni-NTA/SEC-purified gp140$_{UNC}$-Fd-His proteins. The MAb panel tested and the epitopes each MAb recognizes are listed in Table 1. In panel A, data points for multiple non-NAbs are overlapping and circled. Also highlighted is the anomalous binding of the 35O22 bNAb to the 92UG037.8 SOSIP.664-His trimer despite its limited ability to neutralize the corresponding virus (see the text). The data points plotted at MAb concentrations of 30,000 ng/ml in the ELISA or 10,000 ng/ml in the neutralization assay represent values that were endpoints that were not reached in these assays (see Table 1).

tional Env spikes on the Env-pseudotyped viruses, while the gp140$_{UNC}$-Fd-His Env proteins are not.

When we studied the neutralization and ELISA binding data in more detail, we noted that the 35O22 bNAb bound with high affinity to its gp120-gp41$_{ECTO}$ interface epitopes on the 92UG037.8 and CZA97.012 SOSIP.664-His trimers but neutralized the corresponding viruses only partially or not at all, respectively (Table 1 and Fig. 7). Thus, the neutralization curves for 35O22 and 92UG037.8 reached plateau values at ~50%, which implies the existence of a substantial nonneutralized fraction (data not shown). The 35O22 epitope may, in some sequence contexts, be inherently better presented on a soluble trimer than on a membrane-associated version, as suggested previously (23, 66). However, it may be relevant that the structure of the 35O22 epitope on the BG505 SOSIP.664 trimer shows that it probably includes a nonglycosylated form of gp41$_{ECTO}$ residue N625 (23). Other analyses show that on the same trimer, the N625 residue is sometimes glycosylated, sometimes not (48). If virion-associated 92UG037.8 Env proteins are also inconsistently glycosylated at residue N625, that would account for the partial neutralization of this virus by 35O22 that we report here, and likewise for some other viruses that are also incompletely neutralized by this antibody (66). The general subject of why some bNAbs fail to fully neutralize a subset of viruses has recently been discussed in detail (67).

We also observed that various V3-specific non-NAbs neither bound to the 92UG037.8 and CZA97.012 SOSIP.664-His trimers in ELISAs nor neutralized the corresponding viruses. This obser-

vation contrasts with observations of the BG505 and B41 SOSIP.664-D7324 trimers, which do bind the same V3 non-NAbs in ELISAs (18, 28). In a few cases, we did not detect bNAb binding in an ELISA despite observing a binding event in the SPR assay. Examples include PG9, PG16, and PGT145 with CZA97.012 SOSIP.664-His trimers, PGT151 with 92UG037.8 SOSIP.664-His trimers, and 19b with CZA97.012 gp140$_{UNC}$-Fd-His. In all these cases, the SPR profiles show that there is a high rate of bNAb dissociation from the trimers. This propensity to dissociate may account for why these antibodies did not bind detectably in ELISAs; this assay involves extensive washing steps after the antibody-antigen reaction is complete, providing the opportunity for the antibody to dissociate and be washed away.

The binding of 2G12 was partially discrepant between ELISA and SPR assay. This bNAb bound similarly and fairly strongly to the 92UG037.8 SOSIP.664-His trimers and gp140$_{UNC}$-Fd-His proteins in ELISAs, but the maximum signal was twofold higher against the former than the latter in the SPR assay. For both CZA97.012 Env proteins, the ELISA binding signal at the highest input 2G12 concentration was weak and approximately fourfold lower than against 92UG037.8 Env. Accordingly, EC_{50}s were not obtainable (Table 1). Differences in the outcomes of the two assays are probably attributable to the different concentrations of bNAbs used, which are 10-fold higher in the SPR assay than the highest concentration added in the ELISA.

As SOSIP.664 trimers are designed to lack most of the MPER, they do not bind bNAbs against this site. The MPER sequence is
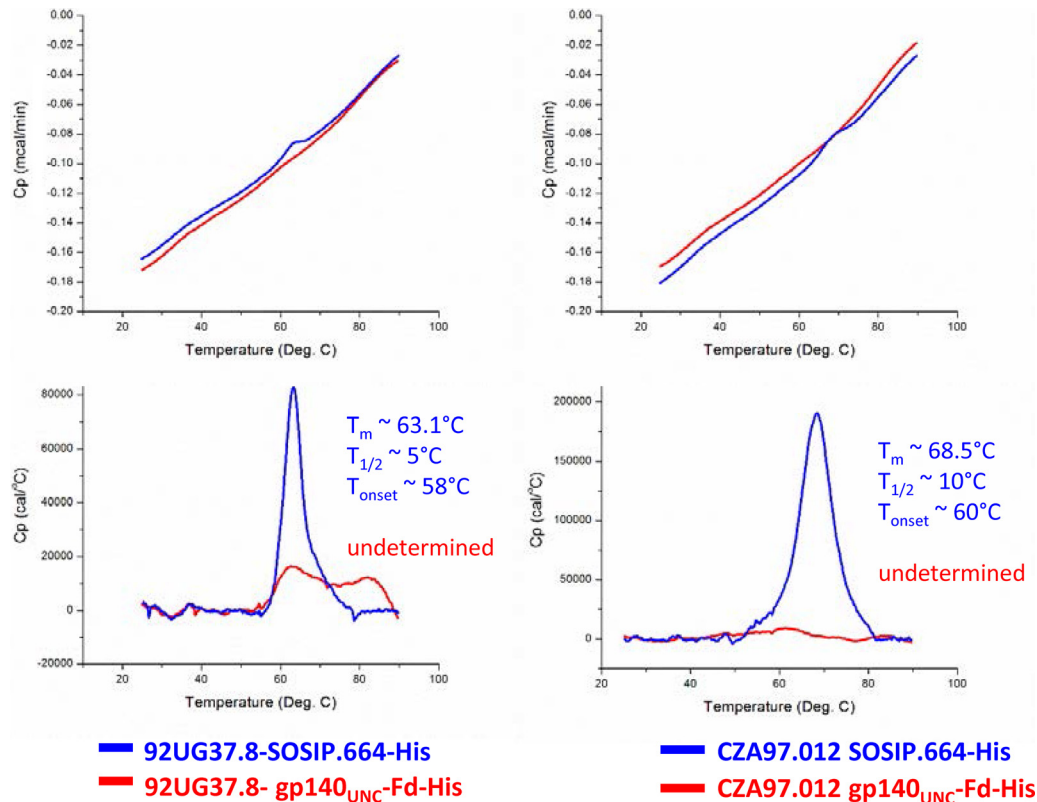
FIG 8 Thermal stability of SOSIP.664-His and gp140_{UNC}-Fd-His proteins. DSC profiles and derivative values are shown for PGT145/SEC-purified 92UG037.8 SOSIP.664-His trimers, PGT151/SEC-purified CZA97.012 SOSIP.664-His trimers, Ni-NTA/SEC-purified 92UG037.8 gp140$_{UNC}$-Fd-His, and CZA97.012 gp140$_{UNC}$-Fd-His proteins. For the SOSIP.664-His trimers, 40 μg was used in each experiment, and for the gp140$_{UNC}$-Fd-His proteins, 60 μg was used. Plots of the raw data are shown in the top panels, and the baseline and molarity-corrected plots are shown in the bottom panels. Derivative values for the SOSIP.664-His trimers were determined by modeling a non-two-state curve over the baseline-corrected data. The corresponding values for the gp140$_{UNC}$-Fd-His proteins could not be determined because clear peaks were not visible in the raw data. Temperature (in degrees Celsius) is shown on the *x* axes of the plots; the crossing point (Cp) (in millicalories or calories per degree) is shown on the *y* axes of the plots. $T_{1/2}$, half-life, T_{onset}, time of onset.

present on the two gp140$_{UNC}$-Fd-His gp140s, but there are several reports that bNAbs against MPER epitopes are unable to bind these proteins (2, 42, 43). We confirmed the lack of binding of the 2F5 and 4E10 bNAbs to the 92UG037.8 and CZA97.012 gp140$_{UNC}$-Fd-His proteins in ELISAs (Table 1).

Thermal stability of SOSIP.664-His and gp140$_{UNC}$-Fd-His proteins. We used DSC to study the thermal stability of the PGT145/SEC-purified 92UG037.8 and PGT151/SEC-purified CZA97.012 SOSIP.664-His trimers and of the Ni-NTA/SEC-purified 92UG037.8 and CZA97.012 gp140$_{UNC}$-Fd-His proteins (Fig. 8). The melting profiles of the 92UG037.8 and CZA97.012 SOSIP.664-His trimers yielded sharp peaks with midpoint temperatures (T_m) of 63.1°C and 68.5°C, respectively. These values approach or are comparable with those previously reported for BG505 SOSIP.664 trimers (T_m, ~67 to 68°C) (68) and indicate that the two new trimers are both homogeneous and highly stable. In contrast, the thermal stability profiles for the gp140$_{UNC}$-Fd-His proteins were highly heterogeneous, to the extent that it was difficult to establish significance with respect to the baseline (Fig. 8, top panels). The most likely explanation of these melting profiles is that there are few preexisting interactions between the individual protomers of the uncleaved gp140s, and hence, little or nothing remains to be denatured as the temperature is increased in the relevant range. Because of the lack of strong intra- and inter-

protomer interactions, denaturation does not occur over a narrow temperature range. Instead, heat is released diffusely over an ~50°C range, which contrasts markedly to what was observed with the SOSIP.664-His trimers (Fig. 8, bottom panels). The absence of a strong melting signal for the gp140$_{UNC}$-Fd-His proteins at temperatures of <100°C may also reflect how their gp41$_{ECTO}$-Fd components have already adopted a conformation similar to the postfusion, six-helix bundle form, which is highly thermostable (4, 69, 70). This point is discussed further below.

Conformational flexibility of SOSIP.664-His and gp140$_{UNC}$-Fd-His proteins. We used HDX-MS to compare the hydrogen/deuterium exchange profiles for the optimally purified gp140 proteins of both designs, a technique that measures the relative solvent accessibility of different regions of proteins (71, 72). Because of sequence variation between the constructs, only a few pepsin-generated peptides could be directly compared between all four 92UG037.8 and CZA97.012 Env proteins (Fig. 9). The comparisons show that the exchange profiles for the 92UG037.8 and CZA97.012 SOSIP.664-His trimers are highly consistent with the previously described BG505 SOSIP.664 trimer with only minor differences arising in V2, V3, and the bridging sheet (48). It is noteworthy that the N- and C-terminal regions of gp120 are strongly protected, which is consistent with their involvement in the β-sheets that link gp120 to gp41$_{ECTO}$ in the prefusion confor-
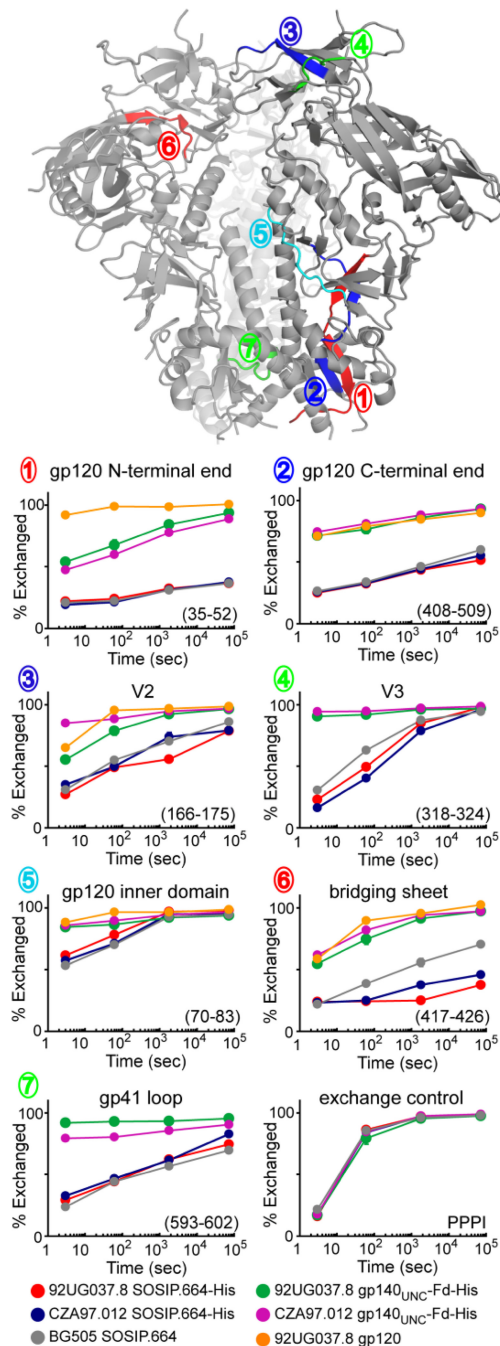
mation of the trimer ([1], [8], [22], [23], [48], [73]). Residues 70 to 83 are not involved in any regular secondary structure but are buried at the gp120-gp41$_{ECTO}$ interface, which accounts for the slight protection observed by HDX (Fig. 9). In contrast, very little protection of the V2, V3, bridging sheet, or gp120-gp41$_{ECTO}$ interface regions was observed in the two gp140$_{UNC}$-Fd-His proteins. Hence, these regions are solvent exposed and not involved in any protective interactions with other Env domains, an outcome similar to those seen in earlier studies of monomeric 92UG037.8 gp120 monomers and various other nonnative gp140 proteins ([41]). The minor protection seen at the gp120 N terminus of the gp140$_{UNC}$-Fd-His proteins was previously observed in nonnative gp140s ([41]) and also in gp120 dimers ([71]).

In the prefusion form of the trimer, residues 593 to 602 of the gp41$_{ECTO}$ loop region are buried and involved in secondary structure, whereas in the postfusion conformation, they become unstructured where they connect the heptad repeat 1 (HR1) and HR2 helices ([48]). The strong protection of this region in both the SOSIP.664-His trimers is consistent with their gp41$_{ECTO}$ components being in the native prefusion conformation (Fig. 9). In marked contrast, the lack of protection of the same region in the two gp140$_{UNC}$-Fd-His gp140s is consistent with the earlier conclusion that the gp41$_{ECTO}$ subunits adopt a conformation resembling the postfusion form; i.e., similar, but perhaps not identical, to the six-helix bundle configuration ([41]).

Glycan compositions of SOSIP.664-His and gp140$_{UNC}$-Fd-His proteins. The glycan compositions of native-like SOSIP.664 trimers and uncleaved gp140 proteins differ markedly ([30], [39], [65]). Specifically, the gp120 subunits of native-like trimers contain a significantly higher percentage of oligomannose glycans as a result of steric constraints on glycan-processing enzymes that are imposed by trimerization, which are similar to the constraints present on virus-associated Env trimers ([30], [39], [65]). In contrast, the same restrictions to glycan processing do not apply to the splayed-out, dissociated subunits of the nonnative uncleaved gp140s, which accordingly contain more highly processed glycans ([39], [65]). Here, we performed similar glycan composition analyses on the 92UG037.8 and CZA97.012 SOSIP.664-His and gp140$_{UNC}$-Fd-His proteins (Table 2 and Fig. 10). As in the above studies, the SOSIP.664-His trimers were purified by the PGT145 or PGT151 bNAb columns followed by SEC, and the gp140$_{UNC}$-Fd-His proteins were purified by Ni-NTA/SEC. Compared to the two uncleaved gp140 proteins, the gp120 subunits of the two SOSIP.664-His trimers had a greater oligomannose content, which is consistent with earlier reports ([30], [39], [65]). The glycans on the gp41$_{ECTO}$ subunits were more highly processed than on their gp120 counterparts, again as reported previously for Env proteins of other genotypes ([39]).

Disulfide bond formation in CZA97.012 SOSIP.664-His and gp140$_{UNC}$-Fd-His proteins. The gp120 proteins from most HIV-1 isolates contain nine intermolecular disulfide bonds that must form for the protein to fold and remain in a native conformation. However, it was reported several years ago that gp120 monomers and uncleaved gp140 proteins contain inappropriate intramolecular disulfide bonds ([53]–[55], [74]). Thus, in at least some fraction of the total population of Env proteins, some Cys residues can pair incorrectly and create nonnative proteins, with the V1V2 loop structure being particularly vulnerable to disulfide bond scrambling. In addition, aberrant disulfides can lead to formation of intermolecular disulfide bonds that cross-link the gp120 sub-

FIG 9 Conformational flexibility of SOSIP.664-His and gp140$_{UNC}$-Fd-His proteins. Deuterium uptake plots are shown for selected peptides from the following purified Env proteins: BG505 SOSIP.664 (gray), 92UG037.8 gp120 (orange), 92UG037.8 SOSIP.664-His (red), CZA97.012 SOSIP.664-His (blue), 92UG037.8 gp140$_{UNC}$-Fd-His (green), and CZA97.012 gp140$_{UNC}$-Fd-His (purple). The position of each peptide is shown on the crystal structure of the BG505 SOSIP.664 trimer (PDB accession no. 4TVP) on the top, with sequence positions shown in parentheses (relative to HXB2 numbering) in the bottom right-hand corner of each graph. Error bars show the standard deviations from duplicate measurements, which in most cases are too small to see. The tetrapeptide (PPPI) was added to each sample to ensure that exchange conditions were identical among all samples compared. The 92UG037.8 and CZA97.012 SOSIP.664-His trimers were purified by the PGT145/SEC and PGT151/SEC methods, respectively, and the two gp140$_{UNC}$-Fd-His proteins were purified via Ni-NTA/SEC. The data for the BG505 SOSIP.664 and 92UG037.8 gp120 proteins were derived from prior reports ([41], [48]).

TABLE 2 Glycan composition of 92UG037.8 and CZA97.012 SOSIP.664-His and gp140_UNC-Fd-His proteins

HIV-1 isolate or genotype and protein[b]	Glycan composition (% of total glycans)[a]					
	M5	M6	M7	M8	M9	Total of M5 to M9
CZA97.012						
gp140_UNC-Fd-His	10	4	7	9	7	37
SOSIP.664-His gp120	7	7	11	21	20	65
SOSIP.664-His gp41	5	5	4	1	0	16
92UG037.8						
gp140_UNC-Fd-His	10	3	6	13	13	46
SOSIP.664-His gp120	14	6	9	14	27	72
SOSIP.664-His gp41	6	4	3	0	0	13
BG505						
WT.SEKS gp140*	6	5	8	12	11	42
SOSIP.664 gp120*	4	4	6	15	34	63
SOSIP.664 gp41*	6	9	12	5	2	34

[a] The data represent the abundance (as a percentage of total glycans) of the oligomannose structures (Man_{5–9}GlcNAc_2; indicated as M5 to M9), individually and in total, for each Env protein analyzed. The remaining glycans are of the complex and hybrid type, similar to what is described in more detail elsewhere for other, similar Env proteins (39). The 92UG037.8 and CZA97.012 gp140_UNC-Fd-His proteins were purified by Ni-NTA/SEC, and the values presented are for the entire gp140 protein (i.e., gp120 plus gp41_ECTO), as it was not possible to separate the individual subunits. The 92UG037.8 SOSIP.664-His trimers were purified by PGT145/SEC, and the CZA97.012 SOSIP.664-His trimers were purified by PGT151/SEC. For these trimers, values are also presented for the individual gp120 and gp41_ECTO subunits, which were separated for analysis on a reducing SDS-polyacrylamide gel.

[b] For comparison, data derived from BG505 Env proteins and published elsewhere (39) are also shown (the proteins are indicated by an asterisk). WT.SEKS is an uncleaved, nonnative gp140 protein similar to gp140_UNC-Fd-His but lacking the Fd and His domains (19). Both BG505 Env proteins were expressed in 293T cells and purified by 2G12/SEC.

units within a gp140 protein or cause these proteins to oligomerize and aggregate (48, 71, 75–77; E. P. Go, A. Cupo, R. P. Ringe, P. Pugach, J. P. Moore, and H. Desaire, unpublished results). As an example of the latter problem, we show that the higher-MW gel bands that are visible in preparations of purified 92UG037.8 and CZA97.012 gp140_UNC-Fd-His proteins are DTT sensitive and, hence, contain disulfide-linked components (Fig. 4B).

Recently, it has been found that native-like BG505 and B41 SOSIP.664 trimers are almost entirely free of scrambled disulfide bonds (Go et al., unpublished). These trimers provided a frame of reference that allowed the estimation of the scrambled disulfide bond content of the corresponding uncleaved gp140s to be in the 20 to 80% range; in other words, 20 to 80% of the gp120 subunits in uncleaved gp140s are aberrantly folded (Go et al., unpublished). Here, we conducted similar analyses of the disulfide bond formation in the PGT151/SEC-purified, native-like CZA97.012 SOSIP.664-His trimer and the Ni-NTA/SEC-purified gp140_UNC-Fd-His protein (Table 3). We also analyzed CZA97.012 SOSIP.664-His trimers purified by lectin/SEC and found that ~50% of the trimers in this preparation adopt native configurations when viewed by EM, compared to >95% for the PGT151/SEC-purified preparation (Fig. 2A).

The canonical disulfide-bonded peptides were detected in each of the three CZA97.012 gp140 populations, which is consistent with several prior reports on various gp120 and gp140 proteins

(53–55, 74). However, aberrant forms were also detected (Table 3). The gp140_UNC-Fd-His protein contained multiple aberrant disulfide bonds affecting the N-terminal region of gp120, which emulates previous results for a different preparation of the same protein (54). In contrast, the SOSIP.664-His trimers contained markedly few aberrant disulfide bonds; in particular, the PGT151/SEC-purified, fully native trimer population was almost completely free of aberrant disulfide bonds, which implies that when these entities are present, they are associated with the nonnative subpopulation of Env trimers (Table 3). Overall, the mass spectrometry signals indicate that the abundance of aberrant disulfide bonds in the PGT151/SEC-purified CZA97.012 SOSIP.664 trimers is 10- to 100-fold lower than in the corresponding gp140_UNC-Fd-His protein. Even when the SOSIP.664 trimers were purified by lectin/SEC, and hence only ~50% native-like, they contained fewer aberrant disulfide bonds than the gp140_UNC-Fd-His protein did (Table 3).

Creation of native-like uncleaved gp140 proteins. Two recent studies report uncleaved gp140s that can adopt native-like configurations, at least in some genotypes, provided a flexible linker of ~10 to 20 residues is introduced between the gp120 and gp41_ECTO subunits (3, 7). The appearance of these single-chain gp140 (sc-gp140) or native flexibly linked gp140 (NFL-gp140) proteins is
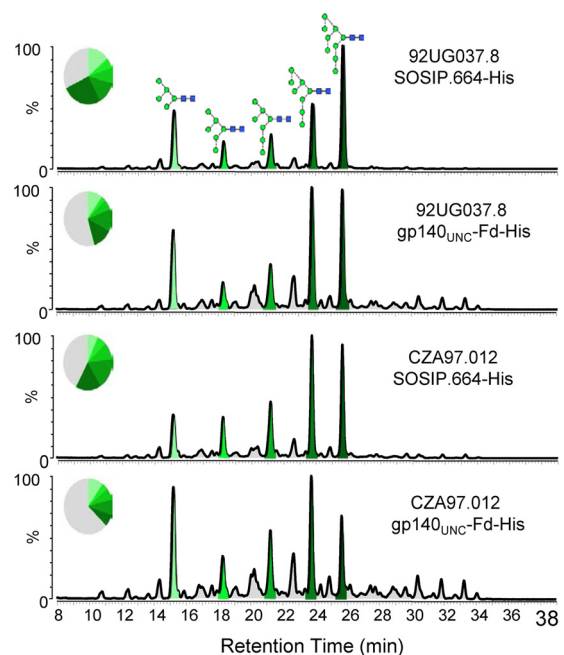

FIG 10 Glycan composition of SOSIP.664-His and gp140_UNC-Fd-His proteins. HILIC-UPLC chromatograms of fluorescently labeled N-linked glycans released from 92UG037.8 and CZA97.012 SOSIP.664-His and gp140_UNC-Fd-His proteins, respectively, purified by the bNAb/SEC and Ni-NTA/SEC methods. The Foldon sequence present in the gp140_UNC-Fd-His proteins does not contain any canonical NXT or NXS motifs, so it is highly unlikely to be glycosylated. Glycans were released from reducing SDS-polyacrylamide gel bands using PNGase F. Peaks corresponding to oligomannose glycans (Man_{5–9}GlcNAc_2) are colored in shades of green; the remaining peaks (gray) correspond to complex and hybrid-type glycans. Peak areas (as a percentage of total glycans) are recorded as numerical values in the associated pie charts and should be consulted to obtain a quantitative estimate of the differences in the glycan contents of the comparator proteins. Glycan structures are depicted according to the color scheme established by the Consortium for Functional Genomics (http://www.functionalglycomics.org/): green circles for mannose and blue squares for N-acetylglucosamine.

TABLE 3 Aberrant disulfide-linked peptides derived from CZA97.012 Env proteins[a]

Disulfide Loop Domain	Disulfide-linked Peptides	CZA97.012 SOSIP.664-His (PGT151/SEC)	CZA97.012 SOSIP.664-His Non-Native (Lectin/SEC)	CZA97.012 gp140$_{UNC}$-Fd-His (Ni-NTA/SEC)
I-II	NDMVDQMHEDIISLWDQSLKPC^{119}VK TTLFC^{54}ASDTK	✗	Minor	✓
	EVHNVWATHAC^{74}VPTDPNPQEIVLED^{88}VTENFNMWK N^{156}C^{157}SFD^{160}TTTEIR	✗	Minor	✓
II	NDMVDQMHEDIISLWDQSLKPC^{119}VK N^{156}C^{157}SFD^{160}TTTEIR	✗	✗	✓
	D^{184}NSD^{187}NSEYILINC^{196}D^{197}ASTITQAC^{205}PK	Trace	✓	✓
	LTPLC^{126}VTLHC^{131}TD^{133}ATFK	Trace	✓	✓
	D^{184}NSD^{187}NSEYILINC^{196}D^{197}ASTITQAC^{205}PK LTPLC^{126}VTLHC^{131}TD^{133}ATFK	✗	✓	✓
III	C^{228}ND^{230}K VNFDPIPIHYC^{218}APAGYAILK	✗	✓	✓
	GPC^{239}ND^{241}VSTVQC^{247}THGIKPVVSTQLLLD^{262}GSLAEK	Trace	Minor	✓
gp41 SOSIP	LIC^{604}C^{605}TNVPWN^{611}SSWSD^{616}K	✓	✓	Not Applicable
	DQQLLGIWGC^{598}SGK VIELKPLGIAPTGC^{598}K	✓	✓	Not Applicable

[a] A checkmark indicates that the disulfide-linked peptide was confirmed to be present, and an x indicates that it was not detected. "Minor" indicates that the peptide was identified but at a much lower abundance compared to that of the gp140$_{UNC}$-Fd-His protein. "Trace" means that the abundance of the peptide was 10- to 100-fold lower than that of the gp140$_{UNC}$-Fd-His protein.

broadly comparable to those of native-like SOSIP.664 trimers when visualized by negative-stain EM. The flexible linker appears to allow the gp120 and gp41$_{ECTO}$ subunits to associate properly, which is not the case with the standard design of uncleaved gp140 (19). However, both the sc-gp140 and NFL-gp140 constructs also include the I559P modification or similar substitutions in gp41$_{ECTO}$ to prevent its transition to the postfusion, six-helix bundle form. In the context of the sc-gp140 protein, introduction of the SOS intersubunit disulfide bond confers additional structural benefits (7). An earlier report on the use of a flexible linker between gp120 and gp41$_{ECTO}$ claims that the resulting uncleaved 92UG037.8 gp140-FL20 proteins are not only native-like but that they are also indistinguishable from the standard gp140$_{UNC}$-Fd-His proteins. Unlike the sc-gp140 or NFL-gp140 trimers, the gp140-FL20 construct does not include either the I559P or the SOS intermolecular disulfide bond (42). As we have shown above that the 92UG037.8 gp140$_{UNC}$-Fd-His protein does not form native-like trimers, we elected to study flexible linker-containing variants that do or do not also incorporate the I559P and SOS changes. The construct designs are shown schematically in Fig. 1.

The 92UG037.8 gp140-FL20 proteins were expressed in 293F cells and purified by the Ni-NTA/SEC method. The SEC profile was similar to that of the 92UG037.8 gp140$_{UNC}$-Fd-His protein, with comparable quantities of aggregates and trimers present (data not shown). Negative-stain EM analysis showed that the gp140-FL20 proteins were indistinguishable from their gp140$_{UNC}$-Fd-His counterparts, with ~95% of the images representing nonnative, structurally aberrant entities (Fig. 11A). SPR antigenicity studies with bNAbs to quaternary structure-dependent or -specific epitopes confirmed the lack of native trimers in the gp140-FL20 preparation. Thus, in contrast to the strong binding of the F105 CD4bs non-NAb, the PG16, PGT145, and 35O22 bNAbs were all nonreactive with the gp140-FL20 proteins (Fig. 11B). Therefore, the addition of the 20-residue flexible linker is not sufficient to convert the 92UG037.8 gp140$_{UNC}$-Fd-His protein into a native-like trimer.

We next investigated the effect of adding the I559P substitution, alone or in combination with the SOS change, to create the 92UG037.8 gp140-FL20-IP and gp140-FL20-SOSIP constructs (Fig. 1). The 293F cell-expressed proteins were purified by Ni-NTA/SEC. Negative-stain EM imaging showed that <5% of the
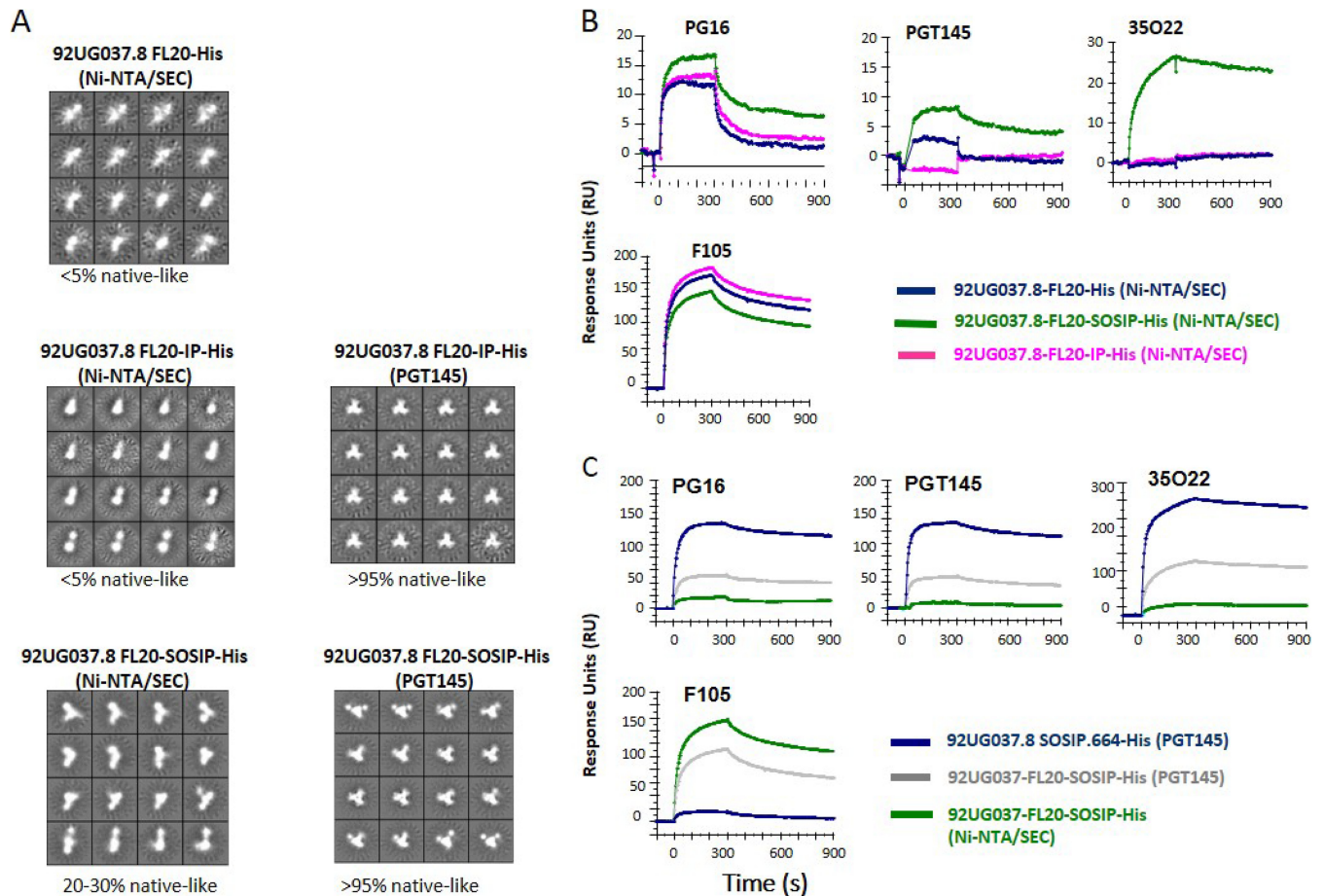
FIG 11 EM and SPR analyses of variants of the 92UG037.8 gp140$_{UNC}$-Fd-His proteins containing flexible linkers. The 92UG037.8 gp140-FL20-His, gp140-FL20-IP-His, and gp140-FL20-SOSIP.664-His constructs are shown in Fig. 1. (A to C) The proteins were purified by the Ni-NTA/SEC method or via a PGT145 bNAb affinity column as indicated and then analyzed by EM (A) or SPR (B and C). (A) The gp140-FL20-His proteins were purified by Ni-NTA/SEC. Attempts to purify native-like trimers based on this construct via the PGT145 column did not yield sufficient protein for EM analysis. The gp140-FL20-IP-His (middle row) and gp140-FL20-SOSIP-His (bottom row) proteins were purified by Ni-NTA/SEC or by the PGT145 affinity column; compared to the Ni-NTA/SEC method, the recoveries of trimers from the PGT145 column were ~5% and ~25%, respectively. (B) SPR data are shown for all three variants of the 92UG037.8 gp140-FL20-His construct, each purified by Ni-NTA/SEC. Each variant is depicted in a different color, as indicated. The quaternary epitope-specific bNAbs PG16 and PGT145 (trimer apex) and 35O22 (gp120-gp41$_{ECTO}$ interface) serve as diagnostic antibodies for assessing the native-like trimer content. The CD4bs non-NAb F105 was used to assess the nonnative Env content of the samples. (C) SPR data were derived using gp140-FL20-SOSIP-His proteins purified either by Ni-NTA/SEC (green) or by a PGT145 affinity column (gray). The PGT145-purified SOSIP.664-His trimer (blue) serves as a comparator for each test antibody.

gp140-FL20-IP proteins adopted a native-like conformation, with the rest being nonnative, while for the gp140-FL20-SOSIP preparation, the native-like trimer percentage increased to the 20 to 30% range (Fig. 11A). When transfection supernatants containing gp140-FL20-IP and gp140-FL20-SOSIP proteins were passed down a PGT145 positive-selection column, small populations of fully native-like trimers could be recovered for EM imaging (Fig. 11A). When a similar experiment was performed using 92UG037.8 gp140$_{UNC}$-Fd-His supernatants, too little Env protein could be recovered from the PGT145 column for EM analysis (data not shown).

The Ni-NTA/SEC-purified gp140-FL20-IP and gp140-FL20-SOSIP proteins were also studied by SPR. The PG16, PGT145, and 35O22 bNAbs did not bind detectably better to the gp140-FL20-IP proteins than to the unmodified gp140$_{UNC}$-Fd-His proteins, indicating that the <5% percentage of native-like trimers shown by

EM was too low to generate quantifiable binding signals in the SPR assay. In contrast, all three of these quaternary structure-dependent or -specific bNAbs bound detectably to the gp140-FL20-SOSIP proteins, most notably for 35O22, with a corresponding reduction in F105 binding (Fig. 11B). Thus, the 20 to 30% of native-like trimers that were visible in EM images of the gp140-FL20-SOSIP proteins also register as native-like structures when their antigenicity was studied by SPR. When the PGT145-purified gp140-FL20-SOSIP trimers were also analyzed by SPR, the binding of the PGT145, PGT16, and 35O22 bNAbs to their quaternary epitopes was increased, while binding of the F105 non-NAb was negligible (Fig. 11C). It was not possible to recover enough gp140-FL20-IP trimers from the PGT145 column for SPR analysis.

We conclude that the I559P change has a minimally positive effect on the structures of the uncleaved gp140-FL20 proteins and

that the SOS intermolecular disulfide bond must also be present to create a meaningful amount of native-like trimers of the 92UG037.8 genotype. However, even the resulting gp140-FL20-SOSIP proteins are predominantly (70 to 80%) nonnative; the residual native-like population can be rescued by positive selection on a PGT145 column. It should be noted that a similar finding was made with the cleaved 92UG037.8 SOSIP.664-His trimers without positive selection, although in that case, the native-like trimer percentage was approximately twofold higher (~50%) (Fig. 2A and 11C).

DISCUSSION

We can draw several conclusions that are relevant to the design and production of soluble Env trimers for structural and vaccine studies. First, fully native-like soluble SOSIP.664 trimers can in fact be derived from the 92UG037.8 and CZA97.012 clade A and clade C *env* genes. In both cases (92UG037.8 and CZA97.012), positive selection for native-like trimers on an affinity column based on a quaternary structure-dependent bNAb (PGT145 and PGT151, respectively) is required to yield a fully native-like trimer preparation, as nonnative trimers are also present when other, less selective purification methods are used. It may be possible to further engineer these *env* sequences to allow a less selective purification method, for example, a 2G12 column, to be used. The present versions of the 92UG037.8 and CZA97.012 SOSIP.664 trimers are fully closed, highly thermally stable and have antigenic properties consistent with their native-like appearance when visualized by negative-stain EM. These trimers therefore add to the repertoire of such reagents that are now available for structural and immunogenicity studies (6, 18, 28, 64).

We again found that the standard design of uncleaved gp140 proteins, in this case, those proteins including a Foldon sequence, yields only nonnative structures as assessed by multiple techniques (3, 7, 16, 19, 26, 30, 41). Thus, the 92UG037.8 and CZA97.012 gp140$_{UNC}$-Fd-His trimer fraction contains disulfide-linked higher-MW aggregates that cannot be fully separated from the nonnative trimers. EM images show that the latter are not true trimers but are oligomeric proteins that contain three splayed-out gp120 subunits linked to a central gp41$_{ECTO}$ core via the uncleaved connecting peptide. The antigenicity data are also consistent with the EM images; nonneutralizing epitopes are exposed on the uncleaved gp140s, but the binding sites for trimer-dependent epitopes are absent. Accordingly, very strong correlations were found between the binding of NAbs or the nonbinding of non-NAbs to the SOSIP.664-His trimers in ELISAs, on the one hand, and on the other hand, neutralization or the lack thereof for the corresponding Env-pseudotyped viruses. In contrast, no correlation was found when a similar analysis was conducted using the gp140$_{UNC}$-Fd-His proteins. The SOSIP.664-His trimers are therefore excellent antigenic mimics of functional Env spikes on viruses, but their uncleaved, disordered, and nonnative counterparts are not.

DSC analysis further reveals that the uncleaved gp140s have, in effect, already lost their native structure prior to the initiation of the melting curves. HDX-MS analysis shows that several regions of the native-like SOSIP.664-His trimers that are involved in secondary structures and that are not solvent exposed behave very differently when they are in the context of the gp140$_{UNC}$-Fd-His proteins. There, the same regions have become solvent accessible, rather than being involved in secondary structural interactions

with other regions of the nonnative oligomers (41, 48). Raising antibodies against such proteins may therefore benefit from the application of new, recently described methods (78). The glycan composition analysis further reinforces how the uncleaved gp140s lack the steric constraints imposed when the gp120 subunits are components of properly assembled trimers; accordingly, the gp140$_{UNC}$-Fd-His glycans are much more highly processed than those on the native-like SOSIP.664-His trimers (39, 79). Finally, the uncleaved CZA97.012 gp140 proteins contain a substantial proportion of gp120 subunits with scrambled disulfide bonds, particularly in the V1V2 region; the aberrant subunits further contribute to the nonnative antigenicity and associated aberrant structural and aggregation properties of these proteins. Based on prior reports and our unpublished work, this problem is generic to the standard design of uncleaved gp140s (e.g., CZA97.012 and 92UG037.8 gp140$_{UNC}$-Fd-His), but it also affects gp120 monomers of multiple genotypes (53–55, 74; Go et al., unpublished). Moreover, the scrambling of disulfide bonds explains why the uncleaved gp140s are prone to forming aggregated, higher-MW forms; internally unpaired Cys residues are available to bond with counterparts on a neighboring gp140 protein. In contrast, the optimally purified (PGT151/SEC), fully native-like CZA97.012 SOSIP.664-His trimers contained very few scrambled disulfide bonds. The latter were, however, found in significant amounts in the lectin/SEC-purified preparation of the same SOSIP.664-His proteins, in which ~50% of the EM images show nonnative trimers. The inference is that, when disulfide bond scrambling occurs, it is incompatible with the formation of a native-like structure, probably because the aberrant gp120 subunits cannot pack properly into the trimer. This topic, and its full implications for Env protein production, will be described more fully elsewhere (Go et al., unpublished).

In all of the above-described assays, there are marked contrasts between the nonnative 92UG037.8 and CZA97.012 gp140$_{UNC}$-Fd-His gp140s and the native-like SOSIP.664-His trimers. The explanation is that the formation of native trimers excludes defective gp120 subunits, creates epitopes for quaternary structure-dependent bNAbs, while occluding those for non-NAbs, and imposes steric constraints on glycan-processing enzymes (1, 8, 20, 22, 23, 39, 68). The various defects present in the 92UG037.8 and CZA97.012 gp140$_{UNC}$-Fd-His gp140s are in no way unique to these genotypes, as they have been found in similar assays using several other uncleaved gp140s and/or can be inferred from the general biochemical properties of such proteins (e.g., the propensity to form disulfide-linked aggregates or the limited reactivity with trimer-specific bNAbs). As various uncleaved gp140s are being tested in or produced for human clinical trials, including proteins based on the 92UG037.8 and CO6980v0c22 genotypes, there are obvious and serious concerns about at least some of the underlying hypotheses (2, 4, 5, 34, 36, 42).

Claims that uncleaved gp140s have native-like properties, including the 92UG037.8 and CZA97.012 gp140$_{UNC}$-Fd-His proteins, are often based on misinterpretation of antigenicity assays, particularly SPR assays (2, 5). In a commonly used SPR format, the gp140s flow over antibodies immobilized on a chip, and a binding reaction is detected. If the test antibody is a bNAb to a quaternary structure-dependent epitope, for example, PGT145, such a binding event is considered to show that the uncleaved gp140 must be a native-like trimer. The interpretation flaw, however, is that the detection of a binding signal says nothing about

the proportion of the input gp140 proteins that express the epitope; all of the gp140 molecules that do not bind the bNAb are invisible in the assay. Thus, an uncleaved gp140 preparation in which, say, 5% of the proteins form native-like trimers, might register as PGT145 reactive in this format of an SPR assay. However, if the same gp140 preparation is used as an immunogen, the bulk of the injected proteins (in this example, 95%) will not be native-like trimers. Our preferred format for SPR involves immobilizing Env proteins on the chip via a His tag and then using the test antibodies in the solution phase. This method allows a precise comparison to be performed between Env proteins of the same or different design, because the same amounts of the comparators can be immobilized. When we directly compared the SOSIP.664-His and gp140$_{UNC}$-Fd-His versions of the 92UG037.8 and CZA97.012 Env proteins in this way, the differences were quantitatively and visually obvious (Fig. 6). Thus, whatever low-level binding of bNAbs, such as PGT145 or PGT151, is observed with the uncleaved gp140s, it is dwarfed by the corresponding signals derived from their native-like SOSIP.664-His counterparts. Here, again, the antigenicity data are entirely consistent with multiple other assays, including EM imaging.

Native-like uncleaved gp140 trimers can indeed be made, but only when a flexible linker is inserted between the gp120 and gp41$_{ECTO}$ subunits and the I559P change, at minimum, is also present (3, 7). We can confirm those findings, as we have produced uncleaved, partially native-like trimers based on the 92UG037.8 genotype. To do so required not only the addition of the flexible linker (in this case, of 20 residues) but also the I559P change and the SOS intermolecular disulfide bond. The I559P change had a detectable although very modest beneficial effect when introduced along with the flexible linker, but the SOS bond was also required to make useful quantities of native-like uncleaved trimers. In the context of the BG505 genotype, the I559P change appears sufficient to confer native-like structure on a uncleaved gp140 containing a flexible linker (3). However, the BG505 *env* sequence is particularly suited to forming native-like trimers, and the quantitative influence of the I559P substitution seems likely to be genotype dependent. It is clear that, by itself, the 20-residue flexible linker is insufficient to convert the nonnative 92UG037.8 gp140$_{UNC}$-Fd-His protein into a native-like trimer. Thus, the resulting 92UG037.8 gp140-FL20 trimer is clearly nonnative when viewed by EM, with antigenicity properties that are consistent with its lack of native structure. Since we made this construct according to the same design reported by Kovacs et al., our findings clearly do not support the claims in that paper that both the 92UG037.8 gp140$_{UNC}$-Fd-His and gp140-FL20 proteins are native-like trimers (42). In fact, we conclude from multiple types of biochemical and biophysical analyses that neither protein is native-like. What is verifiable is the claim that the 92UG037.8 gp140$_{UNC}$-Fd-His and gp140-FL20 proteins are, in effect, identical to one another. Our analyses show, however, that their resemblance is because they both form nonnative trimers.

While the introduction of a flexible linker and SOSIP substitutions allows recognizably native-like uncleaved trimers of the 92UG037.8 genotype to be made, they are present at only 20 to 30% of the total population unless they are enriched via a PGT145 positive-selection column. The same applies to the cleaved 92UG037.8 SOSIP.664-His trimers after 2G12/SEC purification, although in that case, the percentage of native-like

trimers was approximately twofold higher. Whether the 92UG037.8 SOSIP.664-His and gp140-FL20-SOSIP proteins could be further engineered to allow purification of fully native-like trimers (i.e., of BG505 or B41 SOSIP.664 quality) without positive selection remains to be determined.

The compendium of biophysical and biochemical analyses presented here clearly delineates the requirements for producing native-like HIV-1 Env trimers. While each and every assay has limitations and individual data sets need to be carefully interpreted, the combination of several different techniques paints a consistent picture of Env properties. We have noted, in several instances, the potential problems that arise when certain techniques are used in isolation to make what we have now shown are unjustified conclusions about what constitutes a native-like trimer (42). Additionally, as we have shown elsewhere and reinforce here, negative-stain EM is a robust tool; the images that it generates correlate extremely well with the antigenicity and biophysical properties of native-like trimers and nonnative gp140 proteins (18, 19, 28–30). Thus, while it is convenient to claim that SOSIP mutations are responsible for conferring a degree of stability on Env trimers that makes them uniquely amenable to EM analysis (42), stability and homogeneity are exactly what is desirable and sought after in an Env immunogen (6, 80, 81). Moreover, with the SOSIP.664 trimers, protein stability and homogeneity are accompanied by strong antigenicity for bNAb epitopes and promising immunogenicity (18, 28, 29). Finally, we note that if the uncleaved gp140s are truly so fragile that their structure is destroyed by contact with a carbon surface (44), they may be problematic when used as immunogens. How would they behave when they become coated with particulate adjuvants, such as alum, or are exposed to adverse environments like animal or human tissue that contain proteases? Whether or not uncleaved gp140 proteins such as those based on the CZA97.012 and 92UG037.8 genotypes are pursued as immunogens in human clinical trials, claims that these proteins have a native-like structure and, by inference, may be able to induce trimerization-influenced NAbs to tier 2 viruses, are clearly not verifiable. The same concerns apply to other uncleaved gp140s of comparable designs that are also being produced for clinical trials, again on the basis that they mimic the native structure of virion-associated Env (36, 82). A more appropriate rationale for the use of uncleaved gp140s may be their induction of non-NAbs that are partially protective in a macaque challenge model (83). Having said that, it is notable that non-NAbs are clearly very substantially less effective than bNAbs at conferring protection in macaque passive transfer experiments (84–86).

ACKNOWLEDGMENTS

92UG037.8 Env expression plasmids and also the donors of all antibodies used for antigenicity and neutralization analyses.

REFERENCES

1. Lyumkis D, Julien JP, de Val N, Cupo A, Potter CS, Klasse PJ, Burton DR, Sanders RW, Moore JP, Carragher B, Wilson IA, Ward AB. 2013. Cryo-EM structure of a fully glycosylated soluble cleaved HIV-1 envelope trimer. Science **342**:1484–1490. http://dx.doi.org/10.1126/science.1245627.
2. Kovacs JM, Nkolola JP, Peng H, Cheung A, Perry J, Miller CA, Seaman MS, Barouch DH, Chen B. 2012. HIV-1 envelope trimer elicits more potent neutralizing antibody responses than monomeric gp120. Proc Natl Acad Sci U S A **109**:12111–12116. http://dx.doi.org/10.1073/pnas.1204533109.
3. Sharma SK, de Val N, Bale S, Guenaga J, Tran K, Feng Y, Dubrovskaya V, Ward AB, Wyatt RT. 2015. Cleavage-independent HIV-1 Env trimers engineered as soluble native spike mimetics for vaccine design. Cell Rep **11**:539–550. http://dx.doi.org/10.1016/j.celrep.2015.03.047.
4. Nkolola JP, Bricault CA, Cheung A, Shields J, Perry J, Kovacs JM, Giorgi E, van Winsen M, Apetri A, Brinkman-van der Linden EC, Chen B, Korber B, Seaman MS, Barouch DH. 2014. Characterization and immunogenicity of a novel mosaic M HIV-1 gp140 trimer. J Virol **88**:9538–9552. http://dx.doi.org/10.1128/JVI.01739-14.
5. Bricault CA, Kovacs JM, Nkolola JP, Yusim K, Giorgi EE, Shields JL, Perry J, Lavine CL, Cheung A, Ellingson-Strouss K, Rademeyer C, Gray GE, Williamson C, Stamatatos L, Seaman MS, Korber BT, Chen B, Barouch DH. 2015. A multivalent clade C HIV-1 Env trimer cocktail elicits a higher magnitude of neutralizing antibodies than any individual component. J Virol **89**:2507–2519. http://dx.doi.org/10.1128/JVI.03331-14.
6. Sanders RW, van Gils MJ, Derking R, Sok D, Ketas TJ, Burger JA, Ozorowski G, Cupo A, Simonich C, Goo L, Arendt H, Kim HJ, Lee JH, Pugach P, Williams M, Debnath G, Moldt B, van Breemen MJ, Isik G, Medina-Ramirez M, Back JW, Koff WC, Julien JP, Rakasz EG, Seaman MS, Guttman M, Lee KK, Klasse PJ, LaBranche C, Schief WR, Wilson IA, Overbaugh J, Burton DR, Ward AB, Montefiori DC, Dean H, Moore JP. 2015. HIV-1 neutralizing antibodies induced by native-like envelope trimers. Science **349**:aac4223. http://dx.doi.org/10.1126/science.aac4223.
7. Georgiev IS, Joyce MG, Yang Y, Sastry M, Zhang B, Baxa U, Chen RE, Druz A, Lees CR, Narpala S, Schon A, Van Galen J, Chuang GY, Gorman J, Harned A, Pancera M, Stewart-Jones GB, Cheng C, Freire E, McDermott AB, Mascola JR, Kwong PD. 2015. Single-chain soluble BG505.SOSIP gp140 trimers as structural and antigenic mimics of mature closed HIV-1 Env. J Virol **89**:5318–5329. http://dx.doi.org/10.1128/JVI.03451-14.
8. Julien JP, Cupo A, Sok D, Stanfield RL, Lyumkis D, Deller MC, Klasse PJ, Burton DR, Sanders RW, Moore JP, Ward AB, Wilson IA. 2013. Crystal structure of a soluble cleaved HIV-1 envelope trimer. Science **342**:1477–1483. http://dx.doi.org/10.1126/science.1245625.
9. Pantophlet R, Burton DR. 2006. GP120: target for neutralizing HIV-1 antibodies. Annu Rev Immunol **24**:739–769. http://dx.doi.org/10.1146/annurev.immunol.24.021605.090557.
10. Pierson TC, Doms RW. 2003. HIV-1 entry and its inhibition. Curr Top Microbiol Immunol **281**:1–27.
11. Sanders RW, Vesanen M, Schuelke N, Master A, Schiffner L, Kalyanaraman R, Paluch M, Berkhout B, Maddon PJ, Olson WC, Lu M, Moore JP. 2002. Stabilization of the soluble, cleaved, trimeric form of the envelope glycoprotein complex of human immunodeficiency virus type 1. J Virol **76**:8875–8889. http://dx.doi.org/10.1128/JVI.76.17.8875-8889.2002.
12. Leaman DP, Zwick MB. 2013. Increased functional stability and homogeneity of viral envelope spikes through directed evolution. PLoS Pathog **9**:e1003184. http://dx.doi.org/10.1371/journal.ppat.1003184.
13. Nkolola JP, Cheung A, Perry JR, Carter D, Reed S, Schuitemaker H, Pau MG, Seaman MS, Chen B, Barouch DH. 2014. Comparison of multiple adjuvants on the stability and immunogenicity of a clade C HIV-1 gp140 trimer. Vaccine **32**:2109–2116. http://dx.doi.org/10.1016/j.vaccine.2014.02.001.
14. Chakrabarti BK, Feng Y, Sharma SK, McKee K, Karlsson Hedestam GB, Labranche CC, Montefiori DC, Mascola JR, Wyatt RT. 2013. Robust neutralizing antibodies elicited by HIV-1 JRFL envelope glycoprotein trimers in nonhuman primates. J Virol **87**:13239–13251. http://dx.doi.org/10.1128/JVI.01247-13.
15. Forsell MN, Schief WR, Wyatt RT. 2009. Immunogenicity of HIV-1 envelope glycoprotein oligomers. Curr Opin HIV AIDS **4**:380–387. http://dx.doi.org/10.1097/COH.0b013e32832edc19.
16. Tran K, Poulsen C, Guenaga J, de Val N, Wilson R, Sundling C, Li Y, Stanfield RL, Wilson IA, Ward AB, Karlsson Hedestam GB, Wyatt RT. 2014. Vaccine-elicited primate antibodies use a distinct approach to the HIV-1 primary receptor binding site informing vaccine redesign. Proc Natl Acad Sci U S A **111**:E738–E747. http://dx.doi.org/10.1073/pnas.1319512111.
17. Liu J, Bartesaghi A, Borgnia MJ, Sapiro G, Subramaniam S. 2008. Molecular architecture of native HIV-1 gp120 trimers. Nature **455**:109–113. http://dx.doi.org/10.1038/nature07159.
18. Sanders RW, Derking R, Cupo A, Julien JP, Yasmeen A, de Val N, Kim HJ, Blattner C, de la Pena AT, Korzun J, Golabek M, de Los Reyes K, Ketas TJ, van Gils MJ, King CR, Wilson IA, Ward AB, Klasse PJ, Moore JP. 2013. A next-generation cleaved, soluble HIV-1 Env trimer, BG505 SOSIP.664 gp140, expresses multiple epitopes for broadly neutralizing but not non-neutralizing antibodies. PLoS Pathog **9**:e1003618. http://dx.doi.org/10.1371/journal.ppat.1003618.
19. Ringe RP, Sanders RW, Yasmeen A, Kim HJ, Lee JH, Cupo A, Korzun J, Derking R, van Montfort T, Julien JP, Wilson IA, Klasse PJ, Ward AB, Moore JP. 2013. Cleavage strongly influences whether soluble HIV-1 envelope glycoprotein trimers adopt a native-like conformation. Proc Natl Acad Sci U S A **110**:18256–18261. http://dx.doi.org/10.1073/pnas.1314351110.
20. Bartesaghi A, Merk A, Borgnia MJ, Milne JL, Subramaniam S. 2013. Prefusion structure of trimeric HIV-1 envelope glycoprotein determined by cryo-electron microscopy. Nat Struct Mol Biol **20**:1352–1357. http://dx.doi.org/10.1038/nsmb.2711.
21. Harris A, Borgnia MJ, Shi D, Bartesaghi A, He H, Pejchal R, Kang YK, Depetris R, Marozsan AJ, Sanders RW, Klasse PJ, Milne JL, Wilson IA, Olson WC, Moore JP, Subramaniam S. 2011. Trimeric HIV-1 glycoprotein gp140 immunogens and native HIV-1 envelope glycoproteins display the same closed and open quaternary molecular architectures. Proc Natl Acad Sci U S A **108**:11440–11445.
22. Guttman M, Cupo A, Julien JP, Sanders RW, Wilson IA, Moore JP, Lee KK. 2015. Antibody potency relates to the ability to recognize the closed, pre-fusion form of HIV Env. Nat Commun **6**:6144. http://dx.doi.org/10.1038/ncomms7144.
23. Pancera M, Zhou T, Druz A, Georgiev IS, Soto C, Gorman J, Huang J, Acharya P, Chuang GY, Ofek G, Stewart-Jones GB, Stuckey J, Bailer RT, Joyce MG, Louder MK, Tumba N, Yang Y, Zhang B, Cohen MS, Haynes BF, Mascola JR, Morris L, Munro JB, Blanchard SC, Mothes W, Connors M, Kwong PD. 2014. Structure and immune recognition of trimeric pre-fusion HIV-1 Env. Nature **514**:455–461. http://dx.doi.org/10.1038/nature13808.
24. Munro JB, Gorman J, Ma X, Zhou Z, Arthos J, Burton DR, Koff WC, Courter JR, Smith AB, III, Kwong PD, Blanchard SC, Mothes W. 2014. Conformational dynamics of single HIV-1 envelope trimers on the surface of native virions. Science **346**:759–763. http://dx.doi.org/10.1126/science.1254426.
25. Do Kwon Y, Pancera M, Acharya P, Georgiev IS, Crooks ET, Gorman J, Joyce MG, Guttman M, Ma X, Narpala S, Soto C, Terry DS, Yang Y, Zhou T, Ahlsen G, Bailer RT, Chambers M, Chuang GY, Doria-Rose NA, Druz A, Hallen MA, Harned A, Kirys T, Louder MK, O'Dell S, Ofek G, Osawa K, Prabhakaran M, Sastry M, Stewart-Jones GB, Stuckey J, Thomas PV, Tittley T, Williams C, Zhang B, Zhao H, Zhou Z, Donald BR, Lee LK, Zolla-Pazner S, Baxa U, Schon A, Freire E, Shapiro L, Lee KK, Arthos J, Munro JB, Blanchard SC, Mothes W, Binley JM, McDermott AB, Mascola JR, Kwong PD. 2015. Crystal structure, conformational fixation and entry-related interactions of mature ligand-free HIV-1 Env. Nat Struct Mol Biol **22**:522–531. http://dx.doi.org/10.1038/nsmb.3051.
26. Yasmeen A, Ringe R, Derking R, Cupo A, Julien JP, Burton DR, Ward AB, Wilson IA, Sanders RW, Moore JP, Klasse PJ. 2014. Differential binding of neutralizing and non-neutralizing antibodies to native-like soluble HIV-1 Env trimers, uncleaved Env proteins, and monomeric subunits. Retrovirology **11**:41. http://dx.doi.org/10.1186/1742-4690-11-41.
27. Binley JM, Sanders RW, Master A, Cayanan CS, Wiley CL, Schiffner L, Travis B, Kuhmann S, Burton DR, Hu SL, Olson WC, Moore JP. 2002. Enhancing the proteolytic maturation of human immunodeficiency virus type 1 envelope glycoproteins. J Virol **76**:2606–2616. http://dx.doi.org/10.1128/JVI.76.6.2606-2616.2002.
28. Pugach P, Ozorowski G, Cupo A, Ringe R, Yasmeen A, de Val N, Derking R, Kim HJ, Korzun J, Golabek M, de Los Reyes K, Ketas TJ,

Julien JP, Burton DR, Wilson IA, Sanders RW, Klasse PJ, Ward AB, Moore JP. 2015. A native-like SOSIP.664 trimer based on an HIV-1 subtype B env gene. J Virol 89:3380–3395. http://dx.doi.org/10.1128/JVI.03473-14.

29. Derking R, Ozorowski G, Sliepen K, Yasmeen A, Cupo A, Torres JL, Julien JP, Lee JH, van Montfort T, de Taeye SW, Connors M, Burton DR, Wilson IA, Klasse PJ, Ward AB, Moore JP, Sanders RW. 2015. Comprehensive antigenic map of a cleaved soluble HIV-1 envelope trimer. PLoS Pathog 11:e1004767. http://dx.doi.org/10.1371/journal.ppat.1004767.

30. AlSalmi W, Mahalingam M, Ananthaswamy N, Hamlin C, Flores D, Gao G, Rao VB. 2015. A new approach to produce HIV-1 envelope trimers: both cleavage and proper glycosylation are essential to generate authentic trimers. J Biol Chem 290:19780–19795. http://dx.doi.org/10.1074/jbc.M115.656611.

31. Yang X, Farzan M, Wyatt R, Sodroski J. 2000. Characterization of stable, soluble trimers containing complete ectodomains of human immunodeficiency virus type 1 envelope glycoproteins. J Virol 74:5716–5725. http://dx.doi.org/10.1128/JVI.74.12.5716-5725.2000.

32. Yang X, Lee J, Mahony EM, Kwong PD, Wyatt R, Sodroski J. 2002. Highly stable trimers formed by human immunodeficiency virus type 1 envelope glycoproteins fused with the trimeric motif of T4 bacteriophage fibritin. J Virol 76:4634–4642. http://dx.doi.org/10.1128/JVI.76.9.4634-4642.2002.

33. Li Y, O'Dell S, Wilson R, Wu X, Schmidt SD, Hogerkorp CM, Louder MK, Longo NS, Poulsen C, Guenaga J, Chakrabarti BK, Doria-Rose N, Roederer M, Connors M, Mascola JR, Wyatt RT. 2012. HIV-1 neutralizing antibodies display dual recognition of the primary and coreceptor binding sites and preferential binding to fully cleaved envelope glycoproteins. J Virol 86:11231–11241. http://dx.doi.org/10.1128/JVI.01543-12.

34. Nkolola JP, Peng H, Settembre EC, Freeman M, Grandpre LE, Devoy C, Lynch DM, La Porte A, Simmons NL, Bradley R, Montefiori DC, Seaman MS, Chen B, Barouch DH. 2010. Breadth of neutralizing antibodies elicited by stable, homogeneous clade A and clade C HIV-1 gp140 envelope trimers in guinea pigs. J Virol 84:3270–3279. http://dx.doi.org/10.1128/JVI.02252-09.

35. Yang X, Florin L, Farzan M, Kolchinsky P, Kwong PD, Sodroski J, Wyatt R. 2000. Modifications that stabilize human immunodeficiency virus envelope glycoprotein trimers in solution. J Virol 74:4746–4754. http://dx.doi.org/10.1128/JVI.74.10.4746-4754.2000.

36. Wieczorek L, Krebs SJ, Kalyanaraman V, Whitney S, Tovanabutra S, Moscoso CG, Sanders-Buell E, Williams C, Slike B, Molnar S, Dussupt V, Alam SM, Chenine AL, Tong T, Hill EL, Liao HX, Hoelscher M, Maboko L, Zolla-Pazner S, Haynes BF, Pensiero M, McCutchan F, Malek-Salehi S, Cheng RH, Robb ML, VanCott T, Michael NL, Marovich MA, Alving CR, Matyas GR, Rao M, Polonis VR. 2015. Comparable antigenicity and immunogenicity of oligomeric forms of a novel, acute HIV-1 subtype C gp145 envelope for use in preclinical and clinical vaccine research. J Virol 89:7478–7493. http://dx.doi.org/10.1128/JVI.00412-15.

37. Pancera M, Wyatt R. 2005. Selective recognition of oligomeric HIV-1 primary isolate envelope glycoproteins by potently neutralizing ligands requires efficient precursor cleavage. Virology 332:145–156. http://dx.doi.org/10.1016/j.virol.2004.10.042.

38. Si Z, Phan N, Kiprilov E, Sodroski J. 2003. Effects of HIV type 1 envelope glycoprotein proteolytic processing on antigenicity. AIDS Res Hum Retroviruses 19:217–226. http://dx.doi.org/10.1089/088922203763315722.

39. Pritchard LK, Vasiljevic S, Ozorowski G, Seabright GE, Cupo A, Ringe R, Kim HJ, Sanders RW, Doores KJ, Burton DR, Wilson IA, Ward AB, Moore JP, Crispin M. 2015. Structural constraints determine the glycosylation of HIV-1 envelope trimers. Cell Rep 11:1604–1613. http://dx.doi.org/10.1016/j.celrep.2015.05.017.

40. Herrera C, Klasse PJ, Michael E, Kake S, Barnes K, Kibler CW, Campbell-Gardener L, Si Z, Sodroski J, Moore JP, Beddows S. 2005. The impact of envelope glycoprotein cleavage on the antigenicity, infectivity, and neutralization sensitivity of Env-pseudotyped human immunodeficiency virus type 1 particles. Virology 338:154–172. http://dx.doi.org/10.1016/j.virol.2005.05.002.

41. Guttman M, Lee KK. 2013. A functional interaction between gp41 and gp120 is observed for monomeric but not oligomeric, uncleaved HIV-1 Env gp140. J Virol 87:11462–11475. http://dx.doi.org/10.1128/JVI.01681-13.

42. Kovacs JM, Noeldeke E, Ha HJ, Peng H, Rits-Volloch S, Harrison SC, Chen B. 2014. Stable, uncleaved HIV-1 envelope glycoprotein gp140 forms a tightly folded trimer with a native-like structure. Proc Natl Acad Sci U S A 111:18542–18547. http://dx.doi.org/10.1073/pnas.1422269112.

43. Frey G, Peng H, Rits-Volloch S, Morelli M, Cheng Y, Chen B. 2008. A fusion-intermediate state of HIV-1 gp41 targeted by broadly neutralizing antibodies. Proc Natl Acad Sci U S A 105:3739–3744. http://dx.doi.org/10.1073/pnas.0800255105.

44. Dey AK, David KB, Klasse PJ, Moore JP. 2007. Specific amino acids in the N-terminus of the gp41 ectodomain contribute to the stabilization of a soluble, cleaved gp140 envelope glycoprotein from human immunodeficiency virus type 1. Virology 360:199–208. http://dx.doi.org/10.1016/j.virol.2006.09.046.

45. Klasse PJ, Depetris RS, Pejchal R, Julien JP, Khayat R, Lee JH, Marozsan AJ, Cupo A, Cocco N, Korzun J, Yasmeen A, Ward AB, Wilson IA, Sanders RW, Moore JP. 2013. Influences on trimerization and aggregation of soluble, cleaved HIV-1 SOSIP envelope glycoprotein. J Virol 87:9873–9885. http://dx.doi.org/10.1128/JVI.01226-13.

46. Scanlan CN, Ritchie GE, Baruah K, Crispin M, Harvey DJ, Singer BB, Lucka L, Wormald MR, Wentworth P, Jr, Zitzmann N, Rudd PM, Burton DR, Dwek RA. 2007. Inhibition of mammalian glycan biosynthesis produces non-self antigens for a broadly neutralising, HIV-1 specific antibody. J Mol Biol 372:16–22. http://dx.doi.org/10.1016/j.jmb.2007.06.027.

47. Sok D, Doores KJ, Briney B, Le KM, Saye-Francisco KL, Ramos A, Kulp DW, Julien JP, Menis S, Wickramasinghe L, Seaman MS, Schief WR, Wilson IA, Poignard P, Burton DR. 2014. Promiscuous glycan site recognition by antibodies to the high-mannose patch of gp120 broadens neutralization of HIV. Sci Transl Med 6:236ra63. http://dx.doi.org/10.1126/scitranslmed.3008104.

48. Guttman M, Garcia NK, Cupo A, Matsui T, Julien JP, Sanders RW, Wilson IA, Moore JP, Lee KK. 2014. CD4-induced activation in a soluble HIV-1 Env trimer. Structure 22:974–984. http://dx.doi.org/10.1016/j.str.2014.05.001.

49. Zhang Z, Zhang A, Xiao G. 2012. Improved protein hydrogen/deuterium exchange mass spectrometry platform with fully automated data processing. Anal Chem 84:4942–4949. http://dx.doi.org/10.1021/ac300535r.

50. Majumdar R, Manikwar P, Hickey JM, Arora J, Middaugh CR, Volkin DB, Weis DD. 2012. Minimizing carry-over in an online pepsin digestion system used for the H/D exchange mass spectrometric analysis of an IgG1 monoclonal antibody. J Am Soc Mass Spectrom 23:2140–2148. http://dx.doi.org/10.1007/s13361-012-0485-9.

51. Fang J, Rand KD, Beuning PJ, Engen JR. 2011. False EX1 signatures caused by sample carryover during HX MS analyses. Int J Mass Spectrom 302:19–25. http://dx.doi.org/10.1016/j.ijms.2010.06.039.

52. Guttman M, Weis DD, Engen JR, Lee KK. 2013. Analysis of overlapped and noisy hydrogen/deuterium exchange mass spectra. J Am Soc Mass Spectrom 24:1906–1912. http://dx.doi.org/10.1007/s13361-013-0727-5.

53. Go EP, Zhang Y, Menon S, Desaire H. 2011. Analysis of the disulfide bond arrangement of the HIV-1 envelope protein CON-S gp140 DeltaCFI shows variability in the V1 and V2 regions. J Proteome Res 10:578–591. http://dx.doi.org/10.1021/pr100764a.

54. Go EP, Hua D, Desaire H. 2014. Glycosylation and disulfide bond analysis of transiently and stably expressed clade C HIV-1 gp140 trimers in 293T cells identifies disulfide heterogeneity present in both proteins and differences in O-linked glycosylation. J Proteome Res 13:4012–4027. http://dx.doi.org/10.1021/pr5003643.

55. Clark DF, Go EP, Desaire H. 2013. Simple approach to assign disulfide connectivity using extracted ion chromatograms of electron transfer dissociation spectra. Anal Chem 85:1192–1199. http://dx.doi.org/10.1021/ac303124w.

56. Khayat R, Lee JH, Julien JP, Cupo A, Klasse PJ, Sanders RW, Moore JP, Wilson IA, Ward AB. 2013. Structural characterization of cleaved, soluble HIV-1 envelope glycoprotein trimers. J Virol 87:9865–9872. http://dx.doi.org/10.1128/JVI.01222-13.

57. Yang X, Wyatt R, Sodroski J. 2001. Improved elicitation of neutralizing antibodies against primary human immunodeficiency viruses by soluble stabilized envelope glycoprotein trimers. J Virol 75:1165–1171. http://dx.doi.org/10.1128/JVI.75.3.1165-1171.2001.

58. Scanlan CN, Pantophlet R, Wormald MR, Ollmann Saphire E, Stanfield

R, Wilson IA, Katinger H, Dwek RA, Rudd PM, Burton DR. 2002. The broadly neutralizing anti-human immunodeficiency virus type 1 antibody 2G12 recognizes a cluster of alpha1→2 mannose residues on the outer face of gp120. J Virol 76:7306–7321. http://dx.doi.org/10.1128/JVI.76.14.7306 -7321.2002.

59. Murin CD, Julien JP, Sok D, Stanfield RL, Khayat R, Cupo A, Moore JP, Burton DR, Wilson IA, Ward AB. 2014. Structure of 2G12 Fab2 in complex with soluble and fully glycosylated HIV-1 Env by negative-stain single-particle electron microscopy. J Virol 88:10177–10188. http://dx.doi .org/10.1128/JVI.01229-14.

60. Dacheux L, Moreau A, Ataman-Onal Y, Biron F, Verrier B, Barin F. 2004. Evolutionary dynamics of the glycan shield of the human immuno-deficiency virus envelope during natural infection and implications for exposure of the 2G12 epitope. J Virol 78:12625–12637. http://dx.doi.org /10.1128/JVI.78.22.12625-12637.2004.

61. Gray ES, Moore PL, Pantophlet RA, Morris L. 2007. N-linked glycan modifications in gp120 of human immunodeficiency virus type 1 subtype C render partial sensitivity to 2G12 antibody neutralization. J Virol 81: 10769–10776. http://dx.doi.org/10.1128/JVI.01106-07.

62. Duenas-Decamp MJ, Clapham PR. 2010. HIV-1 gp120 determinants proximal to the CD4 binding site shift protective glycans that are targeted by monoclonal antibody 2G12. J Virol 84:9608–9612. http://dx.doi.org /10.1128/JVI.00185-10.

63. Calarese DA, Lee HK, Huang CY, Best MD, Astronomo RD, Stanfield RL, Katinger H, Burton DR, Wong CH, Wilson IA. 2005. Dissection of the carbohydrate specificity of the broadly neutralizing anti-HIV-1 anti-body 2G12. Proc Natl Acad Sci U S A 102:13372–13377. http://dx.doi.org /10.1073/pnas.0505763102.

64. Julien JP, Lee JH, Ozorowski G, Hua Y, de la Peña AT, de Taeye SW, Nieusma T, Cupo A, Yasmeen A, Golabek M, Pugach P, Klasse PJ, Moore JP, Sanders RW, Ward AB, Wilson IA. 2015. Design and struc-ture of two HIV-1 clade C SOSIP.664 trimers that increase the arsenal of native-like Env immunogens. Proc Natl Acad Sci U S A 112:11947–11952. http://dx.doi.org/10.1073/pnas.1507793112.

65. Pritchard LK, Spencer DI, Royle L, Bonomelli C, Seabright GE, Behrens AJ, Kulp DW, Menis S, Krumm SA, Dunlop DC, Crispin DJ, Bowden TA, Scanlan CN, Ward AB, Schief WR, Doores KJ, Crispin M. 2015. Glycan clustering stabilizes the mannose patch of HIV-1 and preserves vulnerability to broadly neutralizing antibodies. Nat Commun 6:7479. http://dx.doi.org/10.1038/ncomms8479.

66. Huang J, Kang BH, Pancera M, Lee JH, Tong T, Feng Y, Imamichi H, Georgiev IS, Chuang GY, Druz A, Doria-Rose NA, Laub L, Sliepen K, van Gils MJ, de la Pena AT, Derking R, Klasse PJ, Migueles SA, Bailer RT, Alam M, Pugach P, Haynes BF, Wyatt RT, Sanders RW, Binley JM, Ward AB, Mascola JR, Kwong PD, Connors M. 2014. Broad and potent HIV-1 neutralization by a human antibody that binds the gp41-gp120 interface. Nature 515:138–142. http://dx.doi.org/10.1038/nature13601.

67. McCoy LE, Falkowska E, Doores KJ, Le K, Sok D, van Gils MJ, Euler Z, Burger JA, Seaman MS, Sanders RW, Schuitemaker H, Poignard P, Wrin T, Burton DR. 2015. Incomplete neutralization and deviation from sigmoidal neutralization curves for HIV broadly neutralizing monoclonal antibodies. PLoS Pathog 11:e1005110. http://dx.doi.org/10.1371/journal .ppat.1005110.

68. Julien JP, Lee JH, Cupo A, Murin CD, Derking R, Hoffenberg S, Caulfield MJ, King CR, Marozsan AJ, Klasse PJ, Sanders RW, Moore JP, Wilson IA, Ward AB. 2013. Asymmetric recognition of the HIV-1 trimer by broadly neutralizing antibody PG9. Proc Natl Acad Sci U S A 110:4351– 4356. http://dx.doi.org/10.1073/pnas.1217537110.

69. Buzon V, Natrajan G, Schibli D, Campelo F, Kozlov MM, Weissenhorn W. 2010. Crystal structure of HIV-1 gp41 including both fusion peptide and membrane proximal external regions. PLoS Pathog 6:e1000880. http: //dx.doi.org/10.1371/journal.ppat.1000880.

70. Lu M, Blacklow SC, Kim PS. 1995. A trimeric structural domain of the HIV-1 transmembrane glycoprotein. Nat Struct Biol 2:1075–1082. http: //dx.doi.org/10.1038/nsb1295-1075.

71. Guttman M, Kahn M, Garcia NK, Hu SL, Lee KK. 2012. Solution structure, conformational dynamics, and CD4-induced activation in full-length, glycosylated, monomeric HIV gp120. J Virol 86:8750–8764. http: //dx.doi.org/10.1128/JVI.07224-11.

72. Rajabi K, Ashcroft AE, Radford SE. 14 March 2015. Mass spectrometric methods to analyze the structural organization of macromolecular com-plexes. Methods http://dx.doi.org/10.1016/j.ymeth.2015.03.004.

73. Ward AB, Wilson IA. 2015. Insights into the trimeric HIV-1 envelope glycoprotein structure. Trends Biochem Sci 40:101–107. http://dx.doi.org /10.1016/j.tibs.2014.12.006.

74. Kassa A, Dey AK, Sarkar P, Labranche C, Go EP, Clark DF, Sun Y, Nandi A, Hartog K, Desaire H, Montefiori D, Carfi A, Srivastava IK, Barnett SW. 2013. Stabilizing exposure of conserved epitopes by structure guided insertion of disulfide bond in HIV-1 envelope glycoprotein. PLoS One 8:e76139. http://dx.doi.org/10.1371/journal.pone.0076139.

75. Owens RJ, Compans RW. 1990. The human immunodeficiency virus type 1 envelope glycoprotein precursor acquires aberrant intermolecular disulfide bonds that may prevent normal proteolytic processing. Virology 179:827– 833. http://dx.doi.org/10.1016/0042-6822(90)90151-G.

76. Hallenberger S, Tucker SP, Owens RJ, Bernstein HB, Compans RW. 1993. Secretion of a truncated form of the human immunodeficiency virus type 1 envelope glycoprotein. Virology 193:510–514. http://dx.doi.org/10 .1006/viro.1993.1156.

77. Finzi A, Pacheco B, Zeng X, Kwon YD, Kwong PD, Sodroski J. 2010. Conformational characterization of aberrant disulfide-linked HIV-1 gp120 dimers secreted from overexpressing cells. J Virol Methods 168: 155–161. http://dx.doi.org/10.1016/j.jviromet.2010.05.008.

78. Sormanni P, Aprile FA, Vendruscolo M. 2015. Rational design of anti-bodies targeting specific epitopes within intrinsically disordered proteins. Proc Natl Acad Sci U S A 112:9902–9907. http://dx.doi.org/10.1073/pnas .1422401112.

79. Go EP, Herschhorn A, Gu C, Castillo-Menendez L, Zhang S, Mao Y, Chen H, Ding H, Wakefield JK, Hua D, Liao HX, Kappes JC, Sodroski J, Desaire H. 2015. Comparative analysis of the glycosylation profiles of membrane-anchored HIV-1 envelope glycoprotein trimers and soluble gp140. J Virol 89:8245–8257. http://dx.doi.org/10.1128 /JVI.00628-15.

80. Crooks ET, Tong T, Chakrabarti B, Narayan K, Georgiev IS, Menis S, Huang X, Kulp D, Osawa K, Muranaka J, Stewart-Jones G, Destefano J, O'Dell S, LaBranche C, Robinson JE, Montefiori DC, McKee K, Du SX, Doria-Rose N, Kwong PD, Mascola JR, Zhu P, Schief WR, Wyatt RT, Whalen RG, Binley JM. 2015. Vaccine-elicited tier 2 HIV-1 neutral-izing antibodies bind to quaternary epitopes involving glycan-deficient patches proximal to the CD4 binding site. PLoS Pathog 11:e1004932. http: //dx.doi.org/10.1371/journal.ppat.1004932.

81. McLellan JS, Chen M, Joyce MG, Sastry M, Stewart-Jones GB, Yang Y, Zhang B, Chen L, Srivatsan S, Zheng A, Zhou T, Graepel KW, Kumar A, Moin S, Boyington JC, Chuang GY, Soto C, Baxa U, Bakker AQ, Spits H, Beaumont T, Zheng Z, Xia N, Ko SY, Todd JP, Rao S, Graham BS, Kwong PD. 2013. Structure-based design of a fusion glycoprotein vaccine for respiratory syncytial virus. Science 342:592–598. http://dx.doi .org/10.1126/science.1243283.

82. Moscoso CG, Xing L, Hui J, Hu J, Kalkhoran MB, Yenigun OM, Sun Y, Paavolainen L, Martin L, Vahlne A, Zambonelli C, Barnett SW, Sriv-astava IK, Cheng RH. 2014. Trimeric HIV Env provides epitope occlu-sion mediated by hypervariable loops. Sci Rep 4:7025. http://dx.doi.org/10 .1038/srep07025.

83. Barouch DH, Alter G, Broge T, Linde C, Ackerman ME, Brown EP, Borducchi EN, Smith KM, Nkolola JP, Liu J, Shields J, Parenteau L, Whitney JB, Abbink P, Ng'ang'a DM, Seaman MS, Lavine CL, Perry JR, Li W, Colantonio AD, Lewis MG, Chen B, Wenschuh H, Reimer U, Piatak M, Lifson JD, Handley SA, Virgin HW, Koutsoukos M, Lorin C, Voss G, Weijtens M, Pau MG, Schuitemaker H. 2015. Protective efficacy of adenovirus-protein vaccines against SIV chal-lenges in rhesus monkeys. Science 349:320–324. http://dx.doi.org/10 .1126/science.aab3886.

84. Burton DR, Hessell AJ, Keele BF, Klasse PJ, Ketas TA, Moldt B, Dunlop DC, Poignard P, Doyle LA, Cavacini L, Veazey RS, Moore JP. 2011. Limited or no protection by weakly or nonneutralizing antibodies against vaginal SHIV challenge of macaques compared with a strongly neutraliz-ing antibody. Proc Natl Acad Sci U S A 108:11181–11186. http://dx.doi .org/10.1073/pnas.1103012108.

85. Moog C, Dereuddre-Bosquet N, Teillaud JL, Biedma ME, Holl V, Van Ham G, Heyndrickx L, Van Dorsselaer A, Katinger D, Vcelar B, Zolla-Pazner S, Mangeot I, Kelly C, Shattock RJ, Le Grand R. 2014. Protective effect of vaginal application of neutralizing and nonneutraliz-ing inhibitory antibodies against vaginal SHIV challenge in macaques. Mucosal Immunol 7:46–56. http://dx.doi.org/10.1038/mi.2013.23.

86. **Santra S, Tomaras GD, Warrier R, Nicely NI, Liao HX, Pollara J, Liu P, Alam SM, Zhang R, Cocklin SL, Shen X, Duffy R, Xia SM, Schutte RJ, Pemble CW, IV, Dennison SM, Li H, Chao A, Vidnovic K, Evans A, Klein K, Kumar A, Robinson J, Landucci G, Forthal DN, Montefiori DC, Kaewkungwal J, Nitayaphan S, Pitisuttithum P, Rerks-Ngarm S, Robb ML, Michael NL, Kim JH, Soderberg KA, Giorgi EE, Blair L, Korber BT, Moog C, Shattock RJ, Letvin NL, Schmitz JE, Moody MA, Gao F, Ferrari G, Shaw GM, Haynes BF.** 2015. Human non-neutralizing HIV-1 envelope monoclonal antibodies limit the number of founder viruses during SHIV mucosal infection in rhesus macaques. PLoS Pathog **11:**e1005042. http://dx.doi.org/10.1371/journal.ppat.1005042.

87. **Walker LM, Phogat SK, Chan-Hui PY, Wagner D, Phung P, Goss JL, Wrin T, Simek MD, Fling S, Mitcham JL, Lehrman JK, Priddy FH, Olsen OA, Frey SM, Hammond PW, Protocol G Principal Investigators, Kaminsky S, Zamb T, Moyle M, Koff WC, Poignard P, Burton DR.** 2009. Broad and potent neutralizing antibodies from an African donor reveal a new HIV-1 vaccine target. Science **326:**285–289. http://dx.doi.org/10.1126/science.1178746.